

Organoaluminum Complexes with Bonds to s-Block, p-Block, d-Block, and f-Block Metal Centers

Stephan Schulz

Abstract This chapter summarizes the recent developments in organoaluminum compounds containing at least one direct bond between aluminum and a s-block, p-block, d-block, or f-block metal center. General synthetic pathways to access such species are described along with their structural and bonding properties.

Keywords σ -Donor · Aluminum · Lewis acid · Lewis base · Molecular intermetallics

Contents

1	Introduction	60
2	Organoaluminum Complexes with s-Block Metals	60
3	Organoaluminum Complexes with p-Block Metals	61
3.1	Organoaluminum Complexes with Group 13 Metals (Ga, In, Tl)	61
3.2	Organoaluminum Complexes with Group 15 Metals (Sb, Bi)	64
3.3	Organoaluminum Complexes with Other p-Block Metals (Sn, Pb, Te)	75
4	Organoaluminum Complexes with d-Block Metals	78
4.1	Synthesis	79
4.2	Structure and Bonding	80
5	Organoaluminum Complexes with f-Block Metals	84
6	Conclusions and Outlook	86
	References	86

Abbreviations

BDE	Bond dissociation energy
Cp	Cyclopentadienyl

S. Schulz (✉)
Institute of Inorganic Chemistry, University of Duisburg-Essen, Universitätsstr. 5-7, 45117 Essen,
Germany
e-mail: stephan.schulz@uni-due.de

Cp*	Pentamethylcyclopentadienyl
Dcpe	1,2-Bis(dicyclohexylphosphanyl)ethane
DFT	Density functional theory
Dipp	2,6-Di- <i>iso</i> -propylphenyl
Dmap	4-Dimethylaminopyridine
dpp-BIAN	1,2-Bis[(2,6-diisopropylphenyl)imino]-acenaphthene
Dvds	1,3-Divinyl-1,1,3,3-tetramethyldisiloxane
MOCVD	Metal organic chemical vapor deposition
Nacnac	β -Diketiminato
Tmeda	Tetramethylethylenediamine
Tmp	Tetramethylpiperidine
Tmpda	Tetramethylpropylenediamine

1 Introduction

Intermetallic complexes have a long standing history in organometallic chemistry not only due to their fascinating structural diversity but also due to their interesting chemical properties. For instance, olefin polymerization reactions using titanium and aluminum complexes as reported by Ziegler and Natta claimed the presence of complexes containing a direct Al–Ti bond. Even though “[Cp₂TiAlEt₂]₂,” a model compound in the Ziegler–Natta olefin polymerization process, was later on shown to form no direct metal–metal bond, the interest in such complexes remained. Since these early studies, homo- and hetero-bimetallic complexes found widespread technological applications in organic synthesis, polymerization catalysis, and were also shown to be very promising *single source precursors* for the deposition of thin films via metal organic chemical vapor deposition (MOCVD) processes. These intermetallic materials (alloys) are also of technical interest since their electrical properties range from metallic to semiconducting (see, for instance, III/V and III/VI materials).

This chapter summarizes the synthesis and structures of intermetallic organoaluminum complexes exhibiting at least one direct bond between aluminum and either main group metals, transition metals, lanthanides, or actinides. Homo-metallic aluminum complexes in lower oxidation states I (AlR)_x and II (Al₂R₄) containing direct Al–Al bonds as well as metalloid cluster complexes are excluded from the present chapter and will be reviewed in Chap. 3 (Low valent organoaluminium (+I, +II) species). In contrast, the synthesis, structure, and bonding properties of donor–acceptor complexes of alanediyIs RAl with group 13 organometallics R'₃M (M = Al, Ga, In) are described in the present contribution.

2 Organoaluminum Complexes with s-Block Metals

Organoaluminum complexes bound to s-group metal centers have been predicted to be stable compounds by computational calculations [1], but alanediyI complexes of alkaline metals and earth alkaline metals remain unknown to date. In contrast,

several gallane complexes have been prepared and structurally characterized [2–6]. Interestingly, dpp-BIAN complexes (dpp-BIAN = 1,2-bis[(2,6-diisopropylphenyl)imino]-acenaphthene) of aluminum and gallium exhibit different coordination modes to alkali metals. While the Ga derivatives form direct Ga–metal bonds [2, 3], the aluminum analogues contain an alkaline metal binding to the π -electronic system of the dpp-BIAN ligand rather than to the Al center [7].

3 Organoaluminum Complexes with p-Block Metals

Heterobimetallic organoaluminum complexes with p-block metals, i.e., group 13 (Ga, In), group 15 (Sb, Bi), and group 16 metals (Te), have been prepared to a large extent. The interest of such complexes does not only lie on their fundamental interest, i.e., the possible formation of Al–E (E = p-block elements) complexes containing multiple bonds [8], but also lie on their potential usefulness in material science. Complexes of group 15 and group 16 metals, for instance, were shown to be promising *single source precursors* for the gas phase deposition of thin films as well as for solution-based synthetic routes to access (nanosized) semiconducting materials such as AlSb and Al₂Te₃.

3.1 Organoaluminum Complexes with Group 13 Metals (Ga, In, Tl)

Homo- and heterobimetallic organoaluminum complexes containing a direct Al–M bond (M = Al, Ga, In) have attracted considerable attention within the last decade due to their interesting bonding properties. They are typically formed by reaction of strong Lewis acidic group 13 complexes M'R₃ with subvalent group 13 metal diyls RM (R = Cp*, nacdac, terphenyl), with the metal center M being in a + I formal oxidation state. Alanedyls RAl and their heavier congeners RM (M = Ga, In) exhibit a singlet electronic ground state with a larger singlet–triplet energy gap for heavier M centers. Group 13 diyls therefore behave as two-electron σ -donors, but also exhibit π -accepting properties as observed in isolobal fragments such as CO, phosphanes PR₃ and singlet carbenes CR₂. The extent of σ -donation and π -acceptance largely depends on the nature of the metal and on the organic group R, even though there is no simple correlation between the nature of the group 13 elements (M and M'), the substituents R, R', and the stability of the complexes RM–M'R₃'. However, the Lewis basicity (σ -donor capacity) of group 13 diyls was found to be higher with increasing π -donor strength of the organic substituent R [9, 10]. As a consequence, strong π -donor ligands such as amido (NR₂) groups and the Cp* substituent enhance the stability of group 13–group 13 donor–acceptor complexes of the type RM–M'R₃ [11]. Simultaneously, the π -acceptor properties of the MR fragment is diminished according to the partial population of the vacant

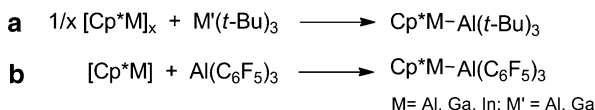


Fig. 1 Synthesis of homo- and heteronuclear group 13-diyl complexes with group 13 Lewis acidic organometallics

p-orbitals of the group 13 metal center through π -donation by the Cp^* substituents. Due to the lack of any back-bonding in intermetallic group 13 element complexes with direct bond to a main group metal, only the σ -donor properties of MR are of interest. In addition, computational calculations demonstrated that the metal–metal bond energies in the corresponding group 13-transition metal complexes also primarily rely on the σ -donor properties of the group 13 diyls as well as on electrostatic contributions [12, 13].

3.1.1 Synthesis

Lewis basic group 13 diyls were found to form stable adducts with group 13 Lewis acids. In particular, heteronuclear complexes containing the strong Lewis acid $\text{B}(\text{C}_6\text{F}_5)_3$, such as $\text{Cp}^*\text{M}-\text{B}(\text{C}_6\text{F}_5)_3$ ($\text{M} = \text{Al}$ [14], Ga [15, 16]), $\text{NacnacM}-\text{B}(\text{C}_6\text{F}_5)_3$ ($\text{Nacnac} = \beta$ -diketiminato, $\text{M} = \text{Al}$ [17], Ga [16]), and $\text{R}'\text{M}-\text{B}(\text{C}_6\text{F}_5)_3$ ($\text{M} = \text{Ga}$, In ; $\text{R}' = \text{terphenyl}$) [18, 19], have been prepared and structurally characterized. The nature of the central M–B bond in these complexes was investigated by computational calculations [12, 20, 21]. In addition, the homoleptic complexes $\text{Cp}^*\text{Al}-\text{Al}(\text{C}_6\text{F}_5)_3$ [22] (Fig. 1), $\text{Cp}^*\text{Al}-\text{Al}(t\text{-Bu})_3$ [23], $\text{Cp}^*\text{Ga}-\text{Ga}(t\text{-Bu})_3$ [15, 23], and $\text{Cp}^*\text{Ga}-\text{Ga}(\text{Cp}^*)\text{X}_2$ ($\text{X} = \text{Cl, I}$) [15] have also been synthesized. These complexes may alternatively be described as valence isomers of the corresponding divalent compounds $\text{R}_2\text{M}-\text{MR}_2$. The nature of the supporting ligands subtly, yet clearly, influences the stability of the resulting complexes as demonstrated by computational calculations [22, 24].

Heteronuclear group 13 bimetallic complexes were formed either by reaction of alanediiyls with group 13 Lewis acids ($\text{Cp}^*\text{Al}-\text{Ga}(t\text{-Bu})_3$ [23]) or that of heavier group 13 diyls congeners with Lewis acidic alanes ($\text{Cp}^*\text{Ga}-\text{Al}(\text{C}_6\text{F}_5)_3$ [25], $\text{Cp}^*\text{Ga}-\text{Al}(t\text{-Bu})_3$ [23], and $\text{Cp}^*\text{In}-\text{Al}(t\text{-Bu})_3$ [23]) (Fig. 1).

3.1.2 Solid State Structures

Selected bond distances and angles for the group 13 complexes discussed above are provided in Table 1. In all these derivatives, the Cp^* ligand in $\text{Cp}^*\text{Al}-\text{MR}_3$ and $\text{Cp}^*\text{M}-\text{AlR}_3$ ($\text{M} = \text{Al, Ga, In}$) adopts a η^5 binding mode to the group 13 metal and the $\text{Cp}^*_{\text{centr}}-\text{M}-\text{M}$ units slightly deviate from linearity. The $\text{M}-\text{Cp}^*_{\text{centr}}$ bond distances of the diyl adducts are significantly shorter than those in the group 13 diyl precursors Cp^*M , as was previously observed for heteronuclear complexes of the type $\text{Cp}^*\text{Al}-\text{BR}_3$ [31]. Such a shortening results from the transformation of

Table 1 Selected bond lengths (Å) and angles (°) for homo- and heterobimetallic group 13 complexes

Adduct	Al–M	M–Cp* _{centr}	Cp*–Al–M	Reference
Cp*Al	–	2.015 ^a /2.063 ^b	–	[26, 27]
Cp*Ga	–	2.081 ^a /2.081 ^b	–	[28, 29]
Cp*In	–	2.302 ^a /2.288 ^b	–	[30]
Cp*Al–B(C ₆ F ₅) ₃	2.169(3)	1.802(3)	172.9	[14]
NacnacAl–B(C ₆ F ₅) ₃	2.183(5)	–	–	[17]
Cp*Al–B(C ₆ F ₅)C ₁₂ F ₈	2.1147(15)	1.782	160.95	[31]
Cp*Al–B(Me)C ₁₂ F ₈	2.149(7)	1.817/1.814	162.76	[31]
Cp*Al–B(Ph)C ₁₂ H ₈	2.1347(13)	1.809	164.12	[31]
Cp*Al–Al(<i>t</i> -Bu) ₃	2.689(2)	1.858	175.0	[23]
Cp*Ga–Al(<i>t</i> -Bu) ₃	2.629(2)	1.913	174.2	[23]
Cp*In–Al(<i>t</i> -Bu) ₃	2.843(2)	2.173	170.0	[23]
Cp*Al–Ga(<i>t</i> -Bu) ₃	2.620(2)	1.861	175.5	[23]
Cp*Al–Al(C ₆ F ₅) ₃	2.591(2)	1.810	170.1	[22]
Cp*Ga–Al(C ₆ F ₅) ₃	2.515(11)	1.810	170.6	[25]

^aAs determined by single crystal X-ray diffraction for [Cp*Al]₄, [Cp*Ga]₆ and [Cp*In]₆^bAs determined by electron diffraction (gas phase) for the monomeric compounds Cp*M

the partially antibonding *electron lone pair* of the diyl Cp*M unit into a donor–acceptor bond upon coordination with MR₃, along with the development of positive (donor-centered) and negative charges (acceptor-centered) at the group 13 metal centers [9].

The intermetallic Al–Al and Ga–Al bond lengths in Cp*M–Al(*t*-Bu)₃ are shorter than the In–Al bond length in Cp*In–Al(*t*-Bu)₃ due to the increased atomic radius of In vs. that of Al and Ga, respectively (Figs. 2 and 3). Moreover, these intermetallic distances are significantly longer than those in Cp*M–Al(C₆F₅)₃ (M = Al, Ga), clearly reflecting the different electronic and steric properties of the R substituents in AlR₃. The shortening of the M–M bond distance when going from Cp*Al–AlR₃ to Cp*Ga–AlR₃ (R = *t*-Bu, C₆F₅) presumably results from stronger electrostatic repulsion in the Al–Al derivative. Thus, upon complexation, the positive charge at the metal atom M(I) increases, with the Al metal donor featuring a larger positive charge compared to the Ga (metal donor) analogue [9]. Interestingly, structural data for NacnacAl–B(C₆F₅)₃ (Nacnac = β-diketiminato, M = Al) [17] agree with the presence of an Al–B donor–acceptor interaction, as expected, along with weak Al...F interactions arising from close intramolecular contacts between one *ortho*-fluorine atom and the Al atom. Therefore, in such a complex, the Janus-type electronic properties of the Al center, a metal center behaving both as a Lewis acid and a Lewis base, is clearly evidenced.

The Lewis basicity of group 13 diyls Cp*M (M = Al, Ga) was investigated by comparing the deviation from planarity of the BC₃ skeleton in Cp*M–B(C₆F₅)₃ complexes following a simple model described by Haaland et al. [32, 33]. According to this structural parameter, Cp*Al is slightly more Lewis basic than Cp*Ga, as may be anticipated. Indeed, the basicity of analogously substituted Lewis bases typically decreases upon going down a given group in the Periodic Table. In fact,

Fig. 2 Solid state structure of $\text{Cp}^*\text{Al-Ga}(t\text{-Bu})_3$

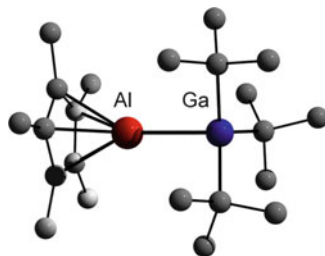
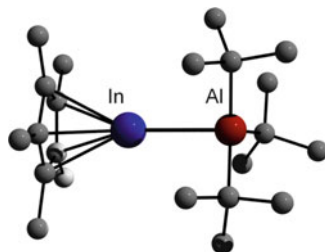


Fig. 3 Solid state structure of $\text{Cp}^*\text{In-Al}(t\text{-Bu})_3$



Cp^*Al was found to be nearly as Lewis basic as PPh_3 . Analogous trends were observed in complexes of the type $\text{Cp}^*\text{M-Al}(t\text{-Bu})_3$ and $\text{Cp}^*\text{M-Ga}(t\text{-Bu})_3$ ($\text{M} = \text{Al}, \text{Ga}, \text{In}$) [23].

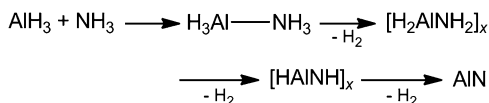
3.2 Organoaluminum Complexes with Group 15 Metals (Sb, Bi)

Compounds containing group 13/15 bonds have a long standing history in main group organometallic chemistry. Apart from their academic interest, such entities are also of interest as novel *single source precursors* for semiconducting III/V material films and nanoparticles via gas phase deposition (MOCVD process) [34–37].

Known for decades, the general reactivity patterns in group 13/15 chemistry have been studied by Wiberg and May. For instance, the reaction of AlH_3 and NH_3 initially yields a Lewis acid–base adduct $\text{H}_3\text{Al-NH}_3$, which then further reacts at elevated temperatures with elimination of H_2 to afford the stepwise and successive formation of aminoalane $[\text{H}_2\text{AlNH}_2]_x$, iminoalane $[\text{HAlNH}]_x$, and aluminum nitride AlN as the final product [38] (Fig. 4).

Since these early studies, numerous compounds of the desired types have been prepared. However, the reaction pathway depicted in Fig. 4 only applies to the synthesis of organoaluminum complexes containing the lighter group 15 elements (N, P, and As). In contrast, access to organoaluminum species of the heavier group 15 elements, such as Sb and Bi, was nearly unknown up to 10 years ago. Nevertheless, ready access to such derivatives has been achieved over the past decade through the exploration and development of novel synthetic strategies.

Fig. 4 Reaction of AlH_3 and NH_3 with stepwise elimination of H_2



3.2.1 Lewis Acid–Base Adducts

The reaction between a Lewis acid group 13 species of the type R_3M and a group 15 Lewis base of the type ER'_3 typically yields the corresponding Lewis acid–base adduct $\text{R}_3\text{M}-\text{ER}'_3$. This reaction, of fundamental interest in main group chemistry, has recently received an increased attention due to the potential use of amine–borane adducts as a hydrogen storage material [39] and to the unusual reactivity of so-called “Frustrated Lewis pairs” [40–42].

The structural properties and general coordination geometries of alane–amine and alane–phosphine adducts have long been studied in the solid state, in solution and in the gas phase [43]. In contrast, the corresponding stibine and bismuthine adducts have only been thoroughly investigated over the past few years [44]. Prior to these studies, the alane–stibine adduct, $\text{Br}_3\text{Al}-\text{SbBr}_3$, a molecular adduct in the gas phase [45] but ionic in the solid state ($[\text{SbBr}_2][\text{AlBr}_4]$) [46], had been synthesized and structurally characterized. Yet, with an enthalpy of formation of $4.3 \pm 0.6 \text{ kJ mol}^{-1}$ [47], $\text{Br}_3\text{Al}-\text{SbBr}_3$ is considered as a weakly bound Lewis acid–base adduct.

The low stability of the alane–stibine and –bismuthine adducts results from the reduced Lewis basicity of stibines and bismuthines due to the increasing s-character of the *electron lone pair* on the group 15 element [48]. However, the Lewis basicity of ER'_3 can be increased via the use of alkyl substituents with a strong electron-donor inductive effect. In addition, sterically demanding substituents, such as *i*-Pr and *t*-Bu, directly affect the Lewis basicity of stibines and bismuthines. Indeed, steric hindrance results in larger C–E–C bond angles thereby decreasing the s-character of the *electron lone pair* and increasing its p-character.

Stable stibine–alane adducts are available by reaction of trialkylstibines SbR'_3 with dialkylchloroalanes R_2AlCl [49] and trialkylalanes AlR_3 [49–53], respectively. Also, the first bismuthine–alane [54, 55], distibine–alane [53, 55–57], and dibismuthine–alane adducts [58] were prepared by reaction of AlR_3 with BiR'_3 , $\text{Sb}_2\text{R}'_4$, and Bi_2Et_4 , respectively, and subsequently structurally characterized (Fig. 5). In most of these adducts, the acid–base interaction in the gas phase and in solution is rather weak. Dissociation enthalpies of *t*-Bu₃Al–E(*i*-Pr)₃ adducts (E = P 12.2 kcal/mol, As 9.9 kcal/mol, Sb 7.8 kcal/mol, Bi 6.9 kcal/mol) [59], as determined by NMR in solution, steadily decrease, as expected, when going to heavier group 15 elements. Such a decrease in bond strength clearly reflects a lower Lewis basicity for heavier group 15 elements.

Table 2 summarizes important structural parameters for alane–stibine and –bismuthine adducts $\text{R}_3\text{Al}-\text{ER}'_3$, while Table 3 features those for distibines and dibismuthines precursors $\text{R}_2\text{E}-\text{ER}'_2$ (E = Sb, Bi) and the corresponding alane adducts.

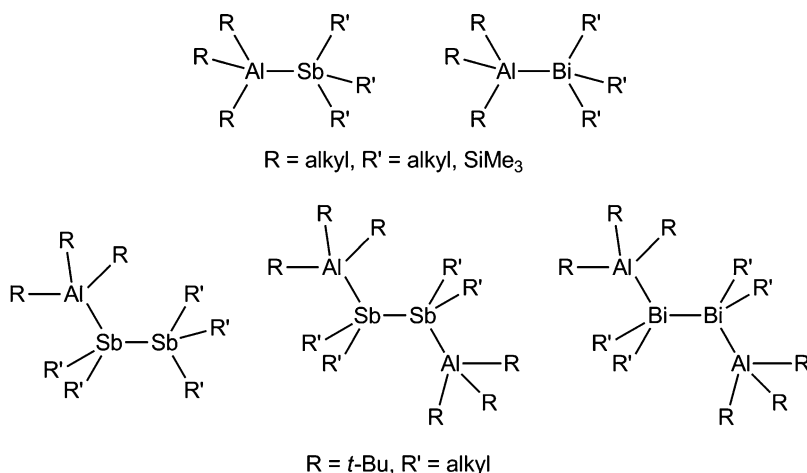


Fig. 5 Coordination modes observed for alane-stibine, distibine, -bismuthine, and dibismuthine adducts

Table 2 Selected bond lengths (Å) and angles (°) for alane-stibine and alane-bismuthine adducts

Adduct	M–E	Al–R (av)	ΣX–E–X	ΣR–Al–R	Reference
R ₃ Al–Sb(SiMe ₃) ₃					
R = Et	2.841(1)	1.984	310.8	347.3	[49]
R = <i>i</i> -Bu	2.848(1)	1.995	312.2	350.5	[50]
R ₂ AlCl–Sb((SiMe ₃) ₃)					
R = <i>t</i> -Bu ^a	2.821(1); 2.798(1)	1.991; 1.994	3.126; 3.091	3.396; 3.415	[49]
R ₃ Al–SbR' ₃					
R = Me; R' = <i>t</i> -Bu	2.834(1)	1.967	319.1	347.2	[51]
R = Et; R' = <i>t</i> -Bu	2.873(1)	1.981	317.8	343.7	[51]
R = <i>t</i> -Bu; R' = Me	2.843(1)	2.020	295.6	349.9	[52]
R = <i>t</i> -Bu; R' = Et	2.845(1)	2.027	301.5	346.9	[51]
R = <i>t</i> -Bu; R' = <i>i</i> -Pr	2.927(1)	2.030	294.1	348.7	[51]
R = <i>t</i> -Bu; R' = <i>i</i> -Bu	2.903(2)	2.019	302.4	347.2	[53]
R ₃ Al–Bi((SiMe ₃) ₃)					
R = Et	2.921(2)	1.978	305.7	350.8	[54]
R ₃ Al–BiR' ₃					
R = <i>t</i> -Bu; R' = Et	2.940(1)	2.011	288.3	351.5	[55]
R = <i>t</i> -Bu; R' = <i>i</i> -Pr	3.088(1)	2.018	286.5	350.4	[54]

^aTwo molecules within the asymmetric unit

In alane-stibine and alane-bismuthine adducts R₃Al–ER'₃, both metal centers generally adopt a distorted tetrahedral coordination geometry with the organic substituents R and R' oriented in a staggered conformation relative to one another. The Al–E bond lengths (E = Sb 2.798(1)–2.927(1) Å; Bi 2.940(1), 3.088(1) Å), strongly dependent on the steric bulk of the organic substituents, are significantly elongated compared to the calculated single bond covalent radii

Table 3 Selected bond lengths (Å) and angles (°) for alane-distibine and alane-dibismuthine adducts

Adduct	E–E	Al–E	Al–C (av.)	E–C (av.)	$\Sigma Y-E-X^a$	$\Sigma C-Al-C$	Reference
E_2R_4							
E = Sb, R = Me	2.862; 2.830(1), 2.838(1)	–	–	2.15(2); 2.156	285.4; 289.4	–	[60, 61]
E = Sb, R = Et	2.8381(5)	–	–	2.170	288.4; 287.6	–	[56]
E = Bi, R = Et	2.9827(7)			2.291	281.8		[56]
$[t-Bu_3Al][E_2R_4]$							
E = Sb, R = <i>i</i> -Pr	2.855(1)	3.003(2)	2.029	2.196	300.9; 288.2	347.4	[55]
$[t-Bu_3Al]_2[E_2R_4]$							
E = Sb, R = Me	2.811(1)	2.919(1)	2.020	2.146	295.1	351.1	[57]
E = Sb, R = Et	2.838(1)	3.001(1)	2.024	2.167	292.9	350.2	[57]
E = Sb, R = <i>n</i> -Pr	2.839(1)	2.964(1)	2.022	2.156	292.2	350.1	[53]
E = Bi, R = Et	2.983(1)	3.084(2)	2.016	2.283	287.7	352.7	[58]

^a $\Sigma Y-E-X = E-E-X_{1,2} + X_1-E-X_2$ (degree of pyramidalization)^b Structural data of the *trans* form

($\Sigma r_{\text{cov}}(\text{AlSb})$: 2.66 Å; $\Sigma r_{\text{cov}}(\text{AlBi})$: 2.77 Å) [62]. In contrast, $\text{Br}_3\text{Al-SbBr}_3$ exhibits a significantly shorter Al–Sb bond length (2.522 Å), less than the sum of the Al and Sb covalent radii.

The longest Al–E bond lengths have been observed for the severely crowded $t\text{-Bu}_3\text{Al-E}(i\text{-Pr})_3$ adducts. The Al–Bi bond lengths are much longer when compared to the Al–Sb bond lengths, a result of the larger atomic radius of Bi. However, the observed difference in $t\text{-Bu}_3\text{Al-E}(i\text{-Pr})_3$ (E = Sb 2.927(1); Bi 3.088(1) Å) exceeds that of their covalent radii (Sb: 1.40, Bi: 1.51 Å) (Figs. 6 and 7).

Tetraalkyldistibines and -dibismuthines typically bind in a bidentated fashion when reacted with AlR_3 Lewis acids, yielding adducts of the type $[\text{R}_3\text{Al}]_2[\text{E}_2\text{R}_4]$ (E = Sb [53, 55, 57], Bi [58], Fig. 8). Only the sterically crowded $i\text{-Pr}_4\text{Sb}_2$ was found to afford the monodentated complex $[t\text{-Bu}_3\text{Al}][\text{Sb}_2(i\text{-Pr})_4]$ (Fig. 9) [55]. These complexes represent the only distibine and dibismuthine complexes of main group metals. These results are strongly related to the already discussed weak Lewis basicity of ER_3 derivatives, and reflect the expressed tendency of tetraalkyldistibines and -dibismuthines to undergo disproportionation reactions with subsequent formation of the respective metal (Sb, Bi) and the corresponding trialkylstibine and -bismuthine R_3E , respectively [63].

The bulky $t\text{-Bu}_3\text{Al}$ groups in the bidentate complexes $[\text{R}_3\text{Al}]_2[\text{E}_2\text{R}_4]$ are, as expected, *trans* to one another for steric reasons. The Al–E bond lengths are

Fig. 6 Solid state structure of $t\text{-Bu}_3\text{Al-Sb}(i\text{-Pr})_3$

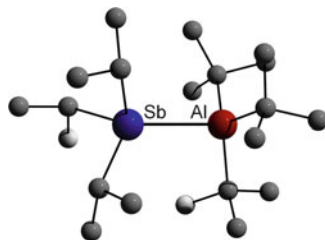


Fig. 7 Solid state structure of $t\text{-Bu}_3\text{Al-Bi}(i\text{-Pr})_3$

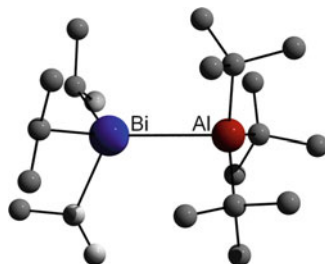


Fig. 8 Solid state structure of $[t\text{-Bu}_3\text{Al}]_2[\text{Bi}_2\text{Et}_4]$

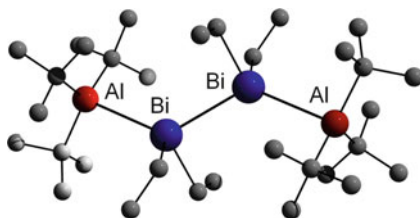
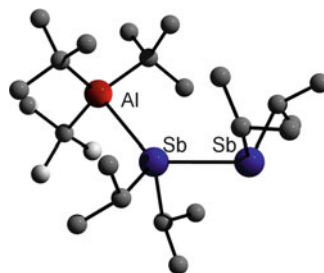


Fig. 9 Solid state structure of $[t\text{-Bu}_3\text{Al}][\text{Sb}_2(i\text{-Pr})_4]$



comparable to those observed in simple trialkylstibine and bismuthine adducts $\text{R}_3\text{Al-ER}'_3$, and the central Sb-Sb and Bi-Bi bond distances are nearly identical to those in distibines and dibismuthines. These structural parameters agree with no E-E bond weakening upon adduct formation, which is consistent with rather weak Lewis acid-base interactions. The sum of the C-Al-C bond angles in $t\text{-Bu}_3\text{Al}$, as estimated from gas phase (electron diffraction, 355.37°) [64] and solid state structural data (355.1° , 355.9° ; 355.5°) [65, 66], is comparable to that in

$[t\text{-Bu}_3\text{Al}]_2[\text{E}_2\text{R}_4]$ (352.7° for the dibismuthine adduct $[t\text{-Bu}_3\text{Al}]_2[\text{B}_2\text{Et}_4]$), further substantiating a weak Lewis acid–base bonding. Moreover, the sum of the C–Sb–C and C–Sb–Sb bond angles is larger in the distibine adducts $[t\text{-Bu}_3\text{Al}]_2[\text{Sb}_2\text{R}_4]$ vs. those in R_4Sb_2 , which points out a partial rehybridization of the Sb centers as expected upon complexation. (The p-character of the electron lone pair is expected to increase and the s-character of the Sb–C and Sb–Sb bonding electron pairs to increase upon complexation, resulting in a widening of the C–Sb–C and C–Sb–Sb bond angles.) In addition, the C–Bi–X ($\text{X} = \text{C}, \text{Bi}$) bond angular sum in dibismuthine adducts $[t\text{-Bu}_3\text{M}]_2[\text{Bi}_2\text{Et}_4]$ lies a bit above that observed in analogously substituted distibine adducts $[t\text{-Bu}_3\text{M}]_2[\text{Sb}_2\text{Et}_4]$. This may be rationalized by a slightly higher p-character for the Bi–C and Bi–Bi bonding electron pairs and an increased s-character for the dative Bi–M bonding electron pairs. Therefore, Bi_2Et_4 has to be considered as a weaker Lewis base than Sb_2Et_4 .

3.2.2 Heterocyclic Complexes $[\text{R}_2\text{AlER}'_2]_x$

Numerous amido-, phosphido-, and arsenide-alanes of the general type $[\text{R}_2\text{AlER}'_2]_x$ ($x = 1, 2, 3$) have been prepared following general and well-established synthetic routes via hydrogen elimination, alkane elimination, salt metathesis, or dehalosilylation reactions (Fig. 10).

The synthetic routes highlighted in Fig. 10, successfully applied to the synthesis of the corresponding Al–P and Al–As heterocycles as well as Ga–Sb and In–Sb heterocycles [71–79], were nevertheless shown to be inappropriate for the synthesis of aluminum heterocycles of the heavier group 15 homologues (Sb and Bi). This finding most likely results from the less acidic properties of the E–H group ($\text{E} = \text{Sb}, \text{Bi}$) along with the well-documented propensity of stibides and bismuthides toward reduction and subsequent formation of elemental Sb and Bi, respectively. Moreover, R_2AlCl and $\text{Sb}(\text{SiMe}_3)_3$ ($\text{R} = \text{Et}, t\text{-Bu}$) were observed not to undergo dehalosilylation as might be anticipated. Instead, the formation of the corresponding Lewis acid–base adducts was observed. In contrast, the reaction of Me_2AlCl with $\text{Sb}(\text{SiMe}_3)_3$ yielded $[\text{Me}(\text{Cl})\text{AlSb}(\text{SiMe}_3)_2]_3$, resulting from the elimination of Me_4Si rather than Me_3SiCl . The different reactivity pattern observed for chloroalanes vs. chlorogallanes and indanes primarily arises from two key characteristics:

1. The Al–Cl bond is stronger than the Ga–Cl and In–Cl bonds [Al–Cl bond (D°_{298} , kJ mol^{-1} : Al–Cl 511 ± 1 ; Ga–Cl 481 ± 13 ; In–Cl 439 ± 8)] [80], disfavoring the elimination of Me_3SiCl .
2. Chloroalanes are stronger Lewis acids than their respective chlorogallanes and -indanes, which favors the formation of Lewis acid–base adducts.

Therefore, novel reaction types had to be developed for the synthesis of heterocyclic complexes $[\text{R}_2\text{AlER}'_2]_x$ ($x = 1, 2, 3$). On that matter, the dehydrosilylation reaction revealed to be an extremely powerful tool [49, 67–70, 81]. Thus, dehydrosilylation reactions (Me_3SiH elimination) can be performed at low

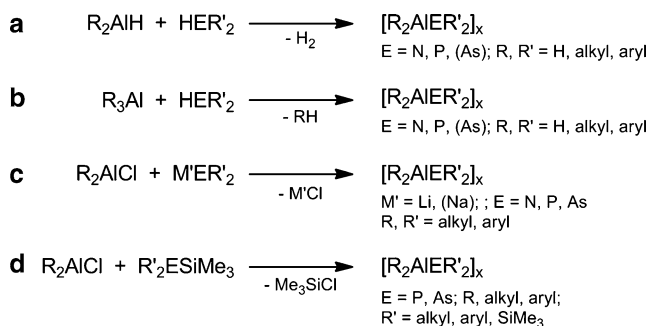


Fig. 10 Hydrogen elimination, alkane elimination, salt metathesis, and dehalosilylation reactions

Table 4 Selected bond lengths (Å) and angles (°) for heterocyclic stibidoalanes and bismuthidoalanes of the general type $[R_2AlER'_2]_x$

Heterocycle	M–E	Al–E–Al	E–Al–E	Reference
$[Me_2AlSb(SiMe_3)_2]_3$	2.703(1)–2.736(1)	118.5(1)–128.2(1)	103.5(1)–106.5(1)	[49]
$[Et_2AlSb(SiMe_3)_2]_2$	2.723(1), 2.729(1)	91.7(1)	88.3(1)	[67]
$[i\text{-Bu}_2AlSb(SiMe_3)_2]_2$	2.743(1), 2.746(1)	93.7(1)	86.3(1)	[67]
$[t\text{-Bu}_2AlSb(SiMe_3)_2]_2$	2.748(1), 2.748(1)	96.1(1)	83.9(1)	[68]
$(Me_2Al)_3(Sb\text{-}Bu_2)_2Sb(SiMe_3)_2$	2.719(2)–2.780(2)	115.4(1)–128.4(1)	103.1(1)–106.9(1)	[69]
$[Me_2AlSb(t\text{-Bu})_2]_3$	2.719(1)–2.784(1)	115.3(1)–128.9(1)	102.8(1)–108.2(1)	[69]
$[t\text{-Bu}_2AlSbEt_2]_2$	2.781(1), 2.786(1)	94.1(1), 94.3(1)	85.8(1)	
$[Me_2AlBi(SiMe_3)_2]_3$	2.755(3)–2.793(3)	121.7(1)–130.5(1)	101.0(1)–104.1(1)	[70]
$[t\text{-Bu}_2AlBi(SiMe_3)_2]_2$	2.840(2)	95.9(1)	84.1(1)	[68]

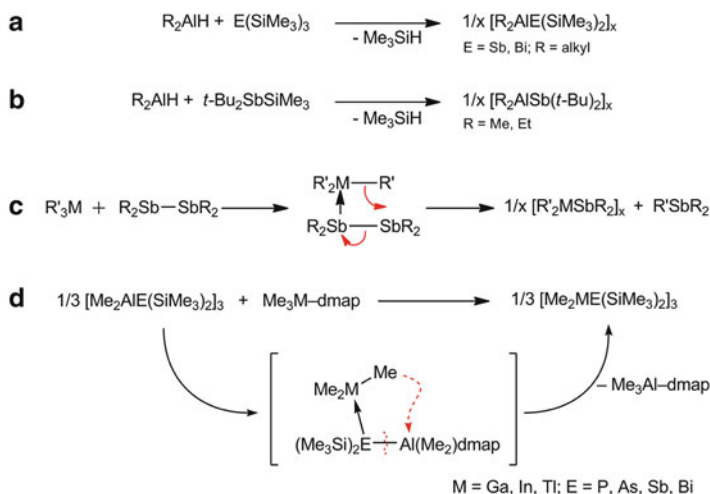
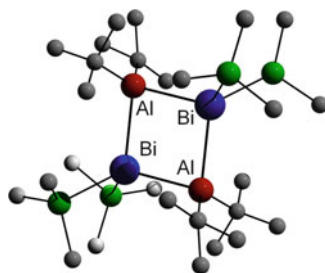


Fig. 11 Dehydrosilylation reaction, distibine cleavage reaction, and metathesis reactions

Fig. 12 Solid state structure of $[t\text{-Bu}_2\text{AlBi}(\text{SiMe}_3)_2]_2$

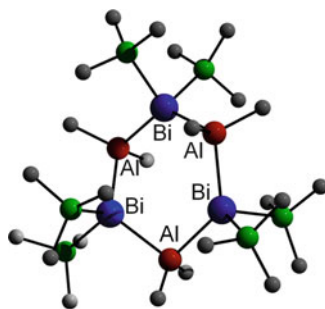


temperatures (0–50°C), allowing the isolation of the as-described heterocycles (frequently very temperature-labile) in very high yields (Fig. 11a, b). It is noteworthy that these preparations can be performed in the absence of any organic solvent, facilitating the isolation of the resulting heterocycles.

Albeit not structurally characterized, $(\text{Cp}^*\text{Al})_3\text{Sb}_2$ was prepared by reaction of $[\text{Cp}^*\text{Al}]_4$ with $[t\text{-BuSb}]_4$ [82]. Also, heterocyclic aluminum-, gallium-, and indium-stibides $[\text{R}_2\text{MSbR}'_2]_x$ were produced via a novel distibine cleavage reaction ([53, 55, 57, 83]; Schulz S, Kuczkowski A et al. unpublished results) (Fig. 11c). On the other hand, a specific metathesis reaction using base-stabilized monomeric Al-pentelides of the type $\text{dmap-AlMe}_2\text{E}(\text{SiMe}_3)_2$ (E = P, As, Sb, Bi; dmap = 4-dimethylaminopyridine) allowed access to the corresponding heterocyclic gallium-, indium-, and thallium-pentelides of the general type $[\text{Me}_2\text{MER}'_2]_x$ (M = Ga, In, Tl; E = P, As, Sb, Bi) [84–86] (for most recent reviews on group 13/15 chemistry of the heavier homologues of group 15 see [87, 88]) (Fig. 11d).

Stibidoalanes $[\text{R}_2\text{AlSbR}'_2]_x$ (R = alkyl, R' = alkyl, SiMe_3) and bismuthidoalanes $[\text{R}_2\text{AlBi}(\text{SiMe}_3)_2]_x$ (R = alkyl) (Fig. 12 and 13) adopt either dimeric or trimeric structures in the solid state, depending on the steric bulk of the organic substituents (Table 4). Analogous findings were previously observed for the lighter group 15 homologues. Sterically demanding substituents favor the formation of four-membered heterocycles, whereas smaller organic substituents yield six-membered heterocycles. Obviously, the nature of the formed heterocycle depends on ring strain and entropy effects. Thus, the formation of six-membered rings relate to the larger Al–E–Al and E–Al–E bond angles that results while entropy effects favor the formation of four-membered rings. Large substituents tend to increase the C–Al–C and C/Si–E–C/Si bond angles; hence the E–Al–E and Al–E–Al angles should be rather small. Thus, in such a case, four-membered rings are more stable than their six-membered ring analogues [89]. In addition, the central group 13 and group 15 elements of analogously substituted heterocycles clearly influence the ring size. The influence of the group 15 element can be seen when comparing Me-substituted heterocycles $[\text{Me}_2\text{AlE}(\text{SiMe}_3)_2]_x$. The phosphido- and arsenidoalanes form four-membered heterocycles, whereas the stibido- and bismuthidoalanes adopt six-membered ring structures. The influence of the group 13 elements is observable in Et-substituted heterocycles $[\text{Et}_2\text{MSb}(\text{SiMe}_3)_2]_x$. Thus, compounds $[\text{Et}_2\text{AlSb}(\text{SiMe}_3)_2]_2$ and $[\text{Et}_2\text{GaSb}(\text{SiMe}_3)_2]_2$ form four-membered rings, whereas $[\text{Et}_2\text{InSb}(\text{SiMe}_3)_2]_3$ adopts a six-membered ring structure (Table 5).

Fig. 13 Solid state structure of $[\text{Me}_2\text{AlBi}(\text{SiMe}_3)_2]_3$

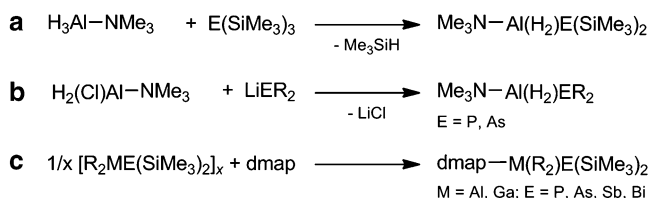


The six-membered heterocycles typically form nonplanar rings in the solid state with distorted twist-boat conformations, in which the Al and Sb/Bi atoms are arranged in distorted tetrahedral environments. The Al–E bond lengths (E = Sb 2.70–2.78 Å, Bi 2.75–2.84 Å) are significantly shorter than those observed in the Lewis acid–base adducts $\text{R}_3\text{Al–ER}'_3$ and $[\textit{t}\text{-Bu}_3\text{Al}]_x[\text{E}_2\text{R}_4]$, respectively, but agree with the calculated single bond covalent radii ($\Sigma r_{\text{cov}}(\text{AlSb})$: 2.66 Å; $\Sigma r_{\text{cov}}(\text{AlBi})$: 2.77 Å) [62]. As may be expected, the exocyclic C–Al–C bond angles strongly depend upon the steric hindrance of the *t*-Bu groups. Sterically demanding substituents thus lead to an opening of the C–Al–C bond angle, in turn decreasing the endocyclic E–Al–E bond angles and increasing the Al–E–Al bond angles.

3.2.3 Monomeric Complexes $\text{dmap–Al}(\text{R}_2)\text{ER}'_2$ and Intermetallic Complexes $\text{dmap–Al}(\text{R}_2)\text{ER}'_2\text{–M}'\text{R}''_n$

While several heterocyclic stibidoalanes or bismuthidoalanes have been prepared and structurally characterized (vide supra), monomeric derivatives $\text{R}_2\text{Al–ER}'_2$ are unknown. In contrast, *base-stabilized* complexes of the general type $\text{dmap–Al}(\text{R}_2)\text{ER}'_2$ were prepared by reaction of the heterocycles $[\text{R}_2\text{AlE}(\text{SiMe}_3)_2]_x$ with strong Lewis bases such as dmap (Fig. 14c) [90–93]. In addition, base-stabilized phosphanyl- and arsanylalanes $\text{Me}_3\text{N–Al}(\text{H}_2)\text{ER}_2$ (E = P, As) are available by a metathetical reaction between the base-stabilized alane $\text{Me}_3\text{N–Al}(\text{H}_2)\text{Cl}$ and LiER_2 (E = P, As; R = Mes = 2,4,6- $\text{Me}_3\text{C}_6\text{H}_2$) (Fig. 14b) [94] and by a dehalosilylation reaction between $\text{H}_3\text{Al–NMe}_3$ and $\text{E}(\text{SiMe}_3)_3$ (E = P, As) (Fig. 14a) [95].

Base-stabilized monomeric compounds feature the shortest Al–E bond lengths observed to date, a likely consequence of the lower coordination number of the group 15 metal center (Table 6). Following an analogous trend earlier mentioned, the degree of pyramidalization of substituted alanes $\text{dmap–Al}(\text{R}_2)\text{E}(\text{SiMe}_3)_2$ (E = P to Bi; R = Me, Et) (Fig. 15) steadily decreases when going to heavier group 15 elements. Similar structural parameters were observed for group 15 triorganyls such as EH_3 , EPh_3 , and EMe_3 . The decreasing bond angles mainly result from an increased *s*-character of the *electron lone pair* on the group 15 element.

**Fig. 14** Synthesis of base-stabilized monomers**Table 5** Average bond lengths (Å) and angles (°) for analogously substituted M–E heterocycles of the general type $[\text{R}_2\text{ME}(\text{SiMe}_3)_2]_x$

M	E	x	M–E	E–M–E	M–E–M	C–M–C	Si–E–Si	Reference
$[\text{Me}_2\text{ME}(\text{SiMe}_3)_2]_x$								
Al	P	2	2.457	89.4	90.6	113.4	108.3	[87, 88]
	As	2	2.536	88.3	91.7	115.0	108.1	[87, 88]
	Sb	3	2.718	104.9	124.0	117.9	101.7	[87, 88]
	Bi	3	2.774	102.3	126.8	119.2	100.5	[87, 88]
Ga	P	2	2.450	88.2	91.8	114.4	108.0	[87, 88]
	As	2	2.530	87.0	93.0	116.8	107.7	[87, 88]
	Sb	3	2.691	105.2	123.6	118.1	101.6	[87, 88]
	Bi	3	2.762	102.0	127.0	120.1	100.3	[81]
In	P	2	2.630	86.7	93.3	116.9	109.8	[87, 88]
	As	2	2.701	85.5	94.5	118.8	109.4	[87, 88]
	Sb	3	2.853	104.1	124.3	120.5	103.0	[87, 88]
	Bi	3	2.915	101.1	127.1	123.0	101.3	[85]
Tl	P	2	2.692	84.5	95.5	122.3	109.0	[85]
	As	2	2.762	93.3	96.7	124.6	108.5	[85]
	Sb	3	2.906	101.7	126.3	127.2	102.3	[86]
$[\text{Et}_2\text{ME}(\text{SiMe}_3)_2]_x$								
Al	P	2	2.457	90.2	89.8	114.6	108.0	[87, 88]
	As	2	2.565	89.6	90.4	115.1	109.3	[87, 88]
	Sb	2	2.726	91.7	88.3	114.5	107.3	[87, 88]
Ga	P	2	2.458	91.4	88.6	113.9	107.8	[87, 88]
	As	2	2.544	92.2	87.8	114.2	107.5	[87, 88]
	Sb	2	2.723	92.7	87.3	114.2	106.9	[87, 88]
In	P	2	2.646	92.5	87.5	114.2	109.1	[87, 88]
	As	2	2.712	93.6	86.4	114.6	108.5	[87, 88]
	Sb	3	2.873	125.1	104.4	116.8	101.2	[87, 88]

The use of strong σ -donor ligands (Lewis bases) has recently been demonstrated to be extremely profitable for the stabilization of unprecedented main group element compounds. Based on the work of Robinson et al., who reported on the synthesis and structure of the carbene-stabilized disilicon complex L-Si=Si-L ($\text{L} = \text{C}[\text{N}(2,6\text{-}i\text{-Pr}_2\text{-C}_6\text{H}_3)\text{CH}]_2$) [96], several elusive compounds including the parent complexes L-HB=BH-L , L-P-P-L and others [97–99], long considered not to be isolable, have been structurally characterized. Moreover, Scheer et al.

Fig. 15 Solid state structure of $\text{dmap-Al(Me}_2\text{)Bi(SiMe}_3\text{)}_2$

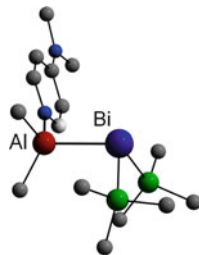


Table 6 Selected bond lengths (Å) and angles (°) of $\text{dmap-M(Me}_2\text{)E(SiMe}_3\text{)}_2$ (M = Al, Ga)

Monomer	M–E	M–N	M–R (av.)	$\Sigma\text{X–E–X}$	Reference
$\text{dmap-Al(Me}_2\text{)P(SiMe}_3\text{)}_2$	2.379(1)	1.984(2)	1.975	309.1	[87, 88]
$\text{dmap-Al(Me}_2\text{)As(SiMe}_3\text{)}_2$	2.472(2)	1.975(4)	1.968	304.1	[87, 88]
$\text{dmap-Al(Et}_2\text{)As(SiMe}_3\text{)}_2$	2.473(1)	1.988(3)	1.977	306.6	[87, 88]
$\text{dmap-Al(Me}_2\text{)Sb(SiMe}_3\text{)}_2$	2.691(1)	1.978(2)	1.970	302.4	[87, 88]
$\text{dmap-Al(Et}_2\text{)Sb(SiMe}_3\text{)}_2$	2.680(1)	1.980(2)	1.980	298.9	[87, 88]
$\text{dmap-Al(Et}_2\text{)Sb}(t\text{-Bu)}_2$	2.708(4)	1.989(2)	1.989	306.8	[93]
$\text{dmap-Al(Me}_2\text{)Bi(SiMe}_3\text{)}_2$	2.755(2)	1.972(4)	1.972	296.8	[87, 88]
$\text{dmap-Al(Et}_2\text{)Bi(SiMe}_3\text{)}_2$	2.750(2)	1.978(5)	1.988	293.4	[87, 88]
$\text{dmap-Ga(Me}_2\text{)P(SiMe}_3\text{)}_2$	2.372(1)	2.080(2)	1.985	305.3	[87, 88]
$\text{dmap-Ga(Me}_2\text{)As(SiMe}_3\text{)}_2$	2.455(1)	2.082(2)	1.982	300.2	[87, 88]
$\text{dmap-Ga(Et}_2\text{)Sb(SiMe}_3\text{)}_2$	2.648(1)	2.066(2)	1.994	298.0	[87, 88]

demonstrated that the coordination of both a Lewis base and a transition metal complex stabilizes highly unstable compounds such as monomeric phosphanylalanes and -gallanes. Thus, compounds $\text{Me}_3\text{N-M(H}_2\text{)PH}_2\text{-W(CO)}_5$ (M = Al, Ga) were produced by a H_2 elimination reaction between $\text{W(CO)}_5\text{PH}_3$ and $\text{Me}_3\text{N-MH}_3$ [100]. According to theoretical calculations, coordination of NMe_3 (108 kJ/mol) and W(CO)_5 (154 kJ/mol) to H_2AlPH_2 stabilizes the monomeric unit by 262 kJ/mol, which is favored over the dimerization of phosphanylalane H_2AlPH_2 (74 kJ/mol).

Comparable compounds of the type $\text{dmap-M(Me}_2\text{)E(SiMe}_3\text{)}_2\text{-M' (CO)}_n$ (M = Al, Ga; E = P, As, Sb; M' = Ni, Fe, Cr) are generally accessible by reaction of the base-stabilized monomers $\text{dmap-M(Me}_2\text{)E(SiMe}_3\text{)}_2$ with transition metal carbonyls such as Ni(CO)_4 , $\text{Fe}_2(\text{CO})_9$, and $(\text{Me}_3\text{N})\text{Cr(CO)}_5$ [101, 102].

For such species, the carbonyl resonances in the ^{13}C -NMR spectra agree with the $\text{dmap-M(Me}_2\text{)E(SiMe}_3\text{)}_2$ moiety being only a weak π -acceptor; hence the phosphorus–transition metal interaction is essentially a P-M' σ -dative bond. According to the synergistic σ -donor/ π -acceptor bonding concept, these findings point toward a slightly higher σ -donor/ π -acceptor ratio when going down to heavier group 15 elements, as reported by Bodner et al. for over 100 transition metal complexes of the general type $\text{R}_3\text{E-M'L}_n$ (E = P, As, Sb) [103]. The observed trends were confirmed by single crystal X-ray diffraction studies, showing an

Fig. 16 Solid state structure of $\text{dmap-Al(Me}_2\text{)Sb(SiMe}_3\text{)}_2\text{-Ga}(t\text{-Bu)}_3$

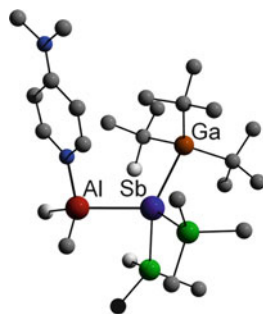


Table 7 Selected bond lengths (Å) and angles (°) of complexes of the type $\text{base-M(R}_2\text{)ER}'_2\text{-M'R}''_n$

Complex	M-E	E-M'	M-N	$\Sigma \text{X-E-Y}$	Reference
$\text{dmap-Al(Me}_2\text{)P(SiMe}_3\text{)}_2\text{-GaMe}_3$	2.428(1)	2.528(1)	1.963(2)	313.5	[84]
$\text{dmap-Al(Me}_2\text{)Sb(SiMe}_3\text{)}_2\text{-Al}(t\text{-Bu)}_3$	2.725(1)	2.869(1)	1.968(3)	298.3	[84]
$\text{dmap-Al(Me}_2\text{)Sb(SiMe}_3\text{)}_2\text{-Ga}(t\text{-Bu)}_3$	2.726(3)	2.889(1)	1.961(7)	298.2	[84]
$\text{Me}_3\text{N-Al(CH}_2\text{SiMe}_3\text{)}_2\text{PPh}_2\text{-Cr(CO)}_5$	2.485(1)	2.482(1)	2.049(3)	308.3	[104]
$\text{Me}_3\text{N-Al(H}_2\text{)PH}_2\text{-W(CO)}_5$	2.367(1)	2.549(1)	2.036(3)		[100]
$\text{Me}_3\text{N-Ga(H}_2\text{)PH}_2\text{-W(CO)}_5$	2.349(2)	2.537(2)	2.039(7)		[100]
$\text{dmap-Al(Me}_2\text{)P(SiMe}_3\text{)}_2\text{-Ni(CO)}_3$	2.400(2)	2.319(2)	1.961(5)	326.0	[101]
$\text{dmap-Al(Me}_2\text{)P(SiMe}_3\text{)}_2\text{-Fe(CO)}_4$	2.432(1)	2.377(1)	1.961(2)	318.9	[101]
$\text{dmap-Al(Me}_2\text{)P(SiMe}_3\text{)}_2\text{-Cr(CO)}_5$	2.428(1)	2.528(1)	1.963(2)	313.5	[101]
$\text{dmap-Al(Me}_2\text{)As(SiMe}_3\text{)}_2\text{-Ni(CO)}_3$	2.479(1)	2.419(1)	1.966(2)	317.7	[102]
$\text{dmap-Al(Me}_2\text{)As(SiMe}_3\text{)}_2\text{-Cr(CO)}_5$	2.512(1)	2.600(1)	1.955(2)	313.0	[101]
$\text{dmap-Al(Me}_2\text{)Sb(SiMe}_3\text{)}_2\text{-Ni(CO)}_3$	2.680(2)	2.556(1)	1.965(4)	314.3	[102]
$\text{dmap-Ga(Me}_2\text{)As(SiMe}_3\text{)}_2\text{-Ni(CO)}_3$	2.465(1)	2.419(1)	2.045(2)	316.3	[101]
$\text{dmap-Ga(Me}_2\text{)Sb(SiMe}_3\text{)}_2\text{-Ni(CO)}_3$	2.647(1)	2.554(1)	2.046(2)	312.8	[101]

increase in the Ni-C bond order and a decrease in the C-O bond order in Ni(CO)_3 -containing complexes vs. Ni(CO)_4 . As reported for the simple Lewis acid-base adducts, the coordination to either a main group metal or a transition metal center typically increases the Si-E-Si and Al-E-Si bond angles, a result of the enhanced p-character of the *electron lone pair*. Analogous tendencies were observed with trialkylalanes and -gallanes analogues $\text{dmap-Al(R}_2\text{)E(SiMe}_3\text{)}_2\text{-MR}_3$ (E = P, Sb; M = Al, Ga) (Fig. 16, Table 7) [84].

3.3 Organoaluminum Complexes with Other p-Block Metals (Sn, Pb, Te)

In sharp contrast to intermolecular complexes with direct Al/group 15 bonds, analogous molecular organoaluminum complexes with bonds to group 14 (Sn, Pb) and group 16 metals (Te) are rather rare. To date, compound $[\text{t-BuNSn}]_4[\text{AlCl}_3]_2$, prepared by reaction of $[\text{t-BuNSn}]_4$ with two equivalents of

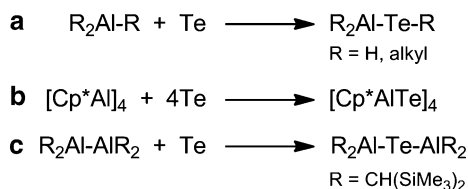
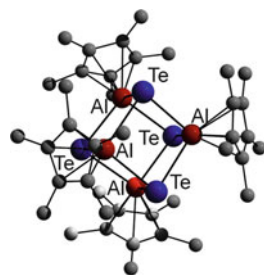


Fig. 17 General reaction pathways for the synthesis of organoaluminum telluride complexes

Fig. 18 Solid state structure of $[\text{Cp}^*\text{AlTe}]_4$

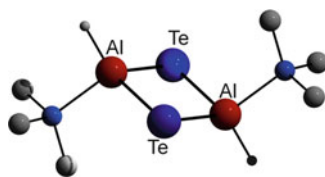


$[\text{AlCl}_3]$, constitutes the only structurally characterized complex containing a dative Sn–Al bond [105]. In addition, the synthesis of $\text{Cp}_2\text{Sn–AlX}_3$ ($\text{X} = \text{Cl, Br}$) was reported [106]. In these complexes, the Sn(II) atom coordinates through its electron lone pair to the Lewis acidic aluminum trihalides.

There are several examples of structurally characterized organoaluminum complexes containing at least one direct Al–Te bond. Such entities are typically prepared by an insertion reaction of elemental Te and an alane derivative containing either an Al–C [107, 108] or an Al–H bond [109–114] (Fig. 17a). Also, the reaction of the subvalent organoaluminum complex $[\text{Cp}^*\text{Al}]_4$ with elemental tellurium was found to proceed via the insertion of Te into the Al–Al bond and formation of the corresponding heterocubane $[\text{Cp}^*\text{AlTe}]_4$ [115] (Fig. 17b). In an analogous manner, the reaction of $[(\text{Me}_3\text{Si})_2\text{CH}]_2\text{Al–Al}[\text{CH}(\text{SiMe}_3)_2]_2$ with elemental tellurium afforded monomeric $[(\text{Me}_3\text{Si})_2\text{CH}]_2\text{Al–Te–Al}[\text{CH}(\text{SiMe}_3)_2]_2$ (Fig. 17c) [116].

The solid state molecular structures of these complexes essentially depend on the sterics of the organic groups (R). Typically, heterocubane-like structures $[\text{RAlTe}]_4$ ($\text{R} = \text{Cp}^*$ [115], Fig. 18, $\text{Me}_2(\text{Et})\text{C}$ [108], $t\text{-Bu}$ [107], and $\text{C}(\text{SiMe}_3)_3$ [111]) were observed. Geometries and thermodynamics of these group 13/16 heterocubanes $[\text{RME}]_4$ ($\text{M} = \text{Al, Ga, In}$; $\text{E} = \text{O, S, Se, Te}$) have also been estimated via DFT studies, suggesting their thermodynamic stability toward fragmentation reactions [117]. Interestingly, treatment of neat $t\text{-Bu}_3\text{Al}$ with two equivalents of elemental tellurium yielded the dimeric complex $[t\text{-Bu}_2\text{AlTe}(t\text{-Bu})]_2$, formally resulting from the insertion of Te into an Al–C bond. Prolonged heating of the latter (toluene, 100°C , 48 h) afforded the heterocubane $[t\text{-BuAlTe}]_4$. Alternatively, $[t\text{-BuAlTe}]_4$ may be formed via a controlled pyrolysis of $[t\text{-Bu}_2\text{AlTe}(t\text{-Bu})]_2$ (300°C , 1 atm) [107].

Dimeric complexes of the type $[\text{RAlTe}]_2$ bearing either a sterically demanding substituent with a side-arm donor [110] or a chelating organic ligand [109, 113]

Fig. 19 Solid state structure of $[\text{Me}_3\text{NAl}(\text{H})(\mu\text{-Te})_2]$ **Table 8** Selected bond lengths (Å) and angles (°) for organoaluminum tellurides

Complex	Al–Te	Te–Al–Te	Al–Te–Al	Reference
$[\text{t-Bu}_2\text{AlTe}(\text{t-Bu})]_2$	2.732(3)	93.9(4)	86.1(4)	[107]
$[\text{Cp}^*\text{AlTe}]_4$	2.7500(9), 2.6883(9), 2.6917(9)	94.84(2), 96.29(2), 94.06(2)	84.86(2), 83.68(2), 85.51(2)	[115]
$[\text{2-(NEt}_2\text{CH}_2\text{)-6-MeC}_6\text{H}_3\text{AlTe}]_2$	2.581(8), 2.588(7)	103.70(3)	76.30(3)	[110]
$[\text{N}(\text{SiMe}_3)\text{C}(\text{Ph})\text{C}(\text{SiMe}_3)_2\text{AlTe}]_2$	2.5619(12), 2.5765(14), 2.5768(14), 2.5753 (12)	103.12(4), 102.79(4)	76.88(4), 77.21(4)	[109]
$\{[\text{HC}\{\text{C}(\text{Me})\text{N}(2,6\text{-}i\text{-Pr}_2\text{C}_6\text{H}_3)\}_2]\text{Al}(\mu\text{-E})\}_2$	2.575(3), 2.581(2)	97.9(1)	82.1(1)	[113]
$[\text{Me}_3\text{N}(\text{PhTe})\text{Al}(\mu\text{-Se})]_2$	2.610(2)	–	–	[118]
$[\text{Me}_3\text{N}(\text{H})\text{Al}(\mu\text{-Te})]_2$	2.586(4), 2.580(4)	103.6(1)	76.4(1)	[114]
$[(\eta^1\text{-3,5-}t\text{-Bu}_2\text{pz}(\mu\text{-Al})\text{H}_2\text{Te})]$	2.5621(12), 2.5763(11)	–	69.41(3)	[112]
$[(\text{Me}_3\text{Si})_2\text{CH}_2\text{Al–Te–Al}[\text{CH}(\text{SiMe}_3)_2]_2]$	2.549(1)	–	110.4(1)	[116]
$\text{Me}_3\text{N–Al}(\text{TePh})_3$	2.589(2), 2.585(2), 2.581(2)	111.21(7), 110.47(8), 110.11(7)	–	[119]

have been prepared. Moreover, the mixed chalcogenide complex *trans*- $[\{\text{Me}_3\text{N}(\text{PhTe})\text{Al}(\mu\text{-Se})\}_2]$, featuring a terminal Al–Te single bond, was synthesized by reaction of *trans*- $[\{\text{Me}_3\text{N}(\text{H})\text{Al}(\mu\text{-Se})\}_2]$ with diphenylditelluride Ph_2Te_2 [118]. The reaction of $\text{Me}_3\text{N–AlH}_3$ with Ph_2Te_2 occurred with Te–Te bond cleavage and hydrogen elimination and subsequent formation of $\text{Me}_3\text{N–Al}(\text{TePh})_3$ [119] (Fig. 19).

Unlike their heavier group 13 counterparts (Ga and In), which have been prepared and structurally characterized (see the following and references cited therein: [120]), examples of monomeric organoaluminum tellurides RAlTe containing an Al=Te double bond have yet to be reported (Table 8).

Apart from being structural curiosities, such Al/Te intermetallic compounds may reveal of interest as single source precursors for the deposition of Al_2Te_3 thin films (via MOCVD), as demonstrated for the Ga and In analogues [121, 122].

4 Organoaluminum Complexes with d-Block Metals

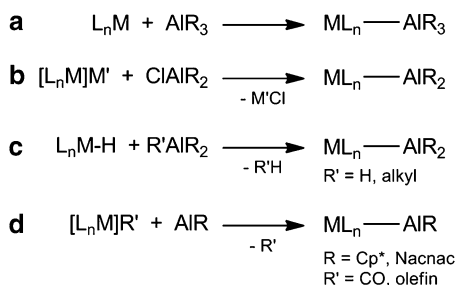
Intermetallic complexes of group 13 metals and transition metals were first investigated by Ziegler and Natta as potentially active complexes in olefin polymerization. The first report on the structural characterization of “[Cp₂TiAlEt₂]₂,” a model compound in the Ziegler–Natta catalytic system, claimed that such a complex contains direct Ti–Al bonds [123]. The latter complex along with others, including [Co₃(CO)₉(μ³-Al)] [124] and [Cp(CO)₃M–AlMe₂] (M = Mo, W) [125, 126], was later unambiguously identified to be an hydride-bridged compound [(C₅H₅)(C₅H₄)Ti(μ-H)AlEt₂]₂ [127] and isocarbonyl-bridged M–CO–Al species, respectively [128–130]. Nevertheless, the interest in this type of intermetallic complexes has remained high since then. Additional impulses came with the development of monovalent group 13 diyls of the type RAl(I), susceptible to act as coordinating Lewis bases toward transition metal complexes. In this area, the report by Robinson et al. on a “ferrogallyne” 2,6-Mes*₂-C₆H₃Ga–Fe(CO)₄ (Mes* = 2,4,6-*i*-Pr₃-C₆H₂) containing a very short Fe–Ga bond (2.2248 Å) [131] thought to be a Fe≡Ga triple bond, promoted a very intense debate, yet sometimes regrettably personal, on the nature of bonding in the latter Fe–Ga complex [132, 133]. These discussions certainly stimulated the general interest in this class of complexes and several group 13-transition metal complexes were synthesized, structurally characterized in the following years and their bonding properties studied by computational calculations.

The unusual coordination properties of the ligands ECp* (E = Al, Ga, In) go beyond their isolobal CO or phosphine analogues. Species of the type ECp* not only stabilize unprecedented cluster structures, but may significantly influence the chemical reactivity of the resulting cluster complexes. By generating very electron rich and thus unusually reactive transition metal centers, unexpected C–H, Si–H, and even C–C bond activation reactions were observed with, for instance, [Ni(AlCp*)₄] [134], [Fe(AlCp*)₅], [Ru(AlCp*)₅] [135], and [RhCp*(CH₃)₂(GaCp*)] [136].

Besides their fascinating bonding properties and unusual reactivity, these intermetallic complexes are of potential interest as single source precursors for the thin film deposition (MOCVD process) of alloys such as β-CoGa [137], CuAl₂ and α/β-CuAl [138], θ-CuE₂ (E = Al, Ga) and Cu_{1-x}Al_x phases [139]. Also, such molecular entities may be useful molecular precursors for nanoparticles synthesis in solution, as reported for α/β-NiAl nanoparticles [140].

The following section summarizes the synthesis, structures, and bonding properties of complexes containing at least one direct transition metal–aluminum bond. The metal derivatives incorporating M–X–M bridging organic groups (X = alkyl, hydride, alkoxides, amides, etc.) are excluded.

Fig. 20 Synthesis of aluminum-transition metal complexes



4.1 Synthesis

Numbers of group 13 diyl-transition metal complexes, mostly with gallanediyls (GaR) derivatives, have been prepared and structurally characterized in the last decade, as reviewed by Fischer and others [141–145]. Several general reaction protocols have been established over the past years for the synthesis of such species. In this domain, early studies mainly dealt with reactions of electron-rich, often anionic, transition metal complexes with triorganylalanes AlR_3 , yielding the corresponding adducts of the type $\text{L}_n\text{M-AlR}_3$, in which the Lewis basic transition metal complex L_nM coordinates to the Lewis-acidic alane AlR_3 [146–149] (Fig. 20a). In addition, salt metathesis reactions between carbonyl metallates and RAlX_2 ($\text{X} = \text{Cl, I}$) [150–153] (Fig. 20b), as well as alkane elimination reactions between transition metal hydrides (containing an acidic M-H function) and alanes [147, 154] (Fig. 20c), have been thoroughly studied.

As initially reported by Schnöckel, substitution reactions between monovalent alanedyl RAl species and transition metal carbonyl olefin complexes certainly constitute the most attractive synthetic approach to access M-Al intermetallic complexes [135, 155–162] (Fig. 20d) [26]. Since then, variously substituted RE species ($\text{E} = \text{Al, Ga, In}$) have been studied, going from sterically bulky alkyl and aryl groups such as terphenyl ligands ($2,4,6\text{-R}_3\text{C}_6\text{H}_2$; $2,4\text{-R}_2\text{C}_6\text{H}_3$) or $\text{Ci}(\text{SiMe}_3)_3$, which are anionic 2-electron substituents, to chelating 4-electron donors such as guanidinato and β -diketiminato-based ligands. The extent of σ -donating and π -accepting properties of these group 13 diyls depends on the nature of the metal center (Al, Ga, In) and the supporting ligand. As a consequence, the structures and chemical properties of the resulting aluminum-transition metal complexes may greatly differ.

In addition to the aforementioned general reaction pathways, complexes containing transition metal–Al bonds have been prepared by rather unusual reactions such as that between $[\text{Cp}^*\text{Co}(\text{C}_2\text{H}_4)_2]$ and $[\text{Et}_2\text{AlH}]$, resulting in the formation of the bimetallic complex $[\{\text{Cp}^*(\eta^2\text{-C}_2\text{H}_4)\text{-Co-Al}(\text{C}_2\text{H}_5)\}_2]$ [163].

Very recently, a Cr(I) aminopyridinate species containing a Cr-Cr quintuple bond was reported to react with AlMe_3 via insertion of the Cr-Cr quintuple bond into the Al-Me bond (carbalumination) to form the trimetallic compound $\text{LCr}(\mu\text{-CH}_3)(\mu\text{-AlMe}_2)\text{CrL}$ ($\text{L} = (2,6\text{-diisopropylphenyl})\text{-[6-(2,6-dimethylphenyl)]-}$

pyridin-2-yl]-amine)[164]. This novel type of complex incorporates a formal Cr–Cr quadruple bond along with formally anionic Me and AlMe₂ groups and features elongated Cr–Al bonds (2.8945(14), 2.9076(14) Å).

4.2 Structure and Bonding

A large variety of intermetallic complexes containing terminal alanes AlR₃, terminal and bridging alanyls AlR₂ as well as terminal and bridging alanediyIs AlR have been structurally characterized (see Table 9).

As stated above, alane complexes of the type L_nM–AlR₃ have typically been prepared via reaction between Lewis basic transition metal carbonyl complexes and AlR₃. The formation of a direct M–Al bond or an isocyanate-bridge M–CO–Al strongly depends on the Lewis basicity of the transition metal complex [146]. Comparisons of structural parameters for complexes containing the same metal centers may not be that meaningful given the limited number of structurally characterized complexes. However, the M–Al bond lengths of *alane complexes* L_nM–AlR₃ such as anionic [Cp(CO)₂Fe–AlPh₃][−] (2.510(2) Å) were observed to be slightly longer than those of *alanylene complexes* L_nM–AlR₂ containing terminally bonded alanyl moieties (e.g., [Cp(CO)₂Fe–Al(tmp)₂] 2.450(1) Å, [(η⁵-C₅H₅)(CO)₂Fe–Al(CH₂)₃NMe₂]*i*-Bu] 2.456(1) Å) and in *alylene complexes* with bridging alanediyI groups [L_nM]₂ μ²–AlR (e.g., [CpFe(CO)₂]₂Al(2-Me₂NCH₂C₆H₄)] 2.468(1), 2.496(1) Å). Homoleptic M(AlR)_x and heteroleptic *alylene complexes* L_nM–AlR with terminal alanediyI groups such as [Fe(AlCp*)₅] and [(CO)₄Fe(AlCp*)] typically show significantly shorter intermetallic bonds. The only exception was observed for the alane complex (Cy₃P)₂Pt–AlCl₃ (2.3857(7) Å) (Fig. 21), whose Pt–Al bond length is comparable to those observed in the alylene complexes with terminal alanediyI moiety [(dcpe)Pt(AlCp*)₂] (dcpe = 1,2-bis(dicyclohexylphosphanyl)ethane), 2.327(2), 2.335(2) Å).

The bonding situation in L_nM–AlR₃ is best described as that of a simple adduct between the Lewis-basic transition metal complex coordinated to the Lewis-acidic alane, as shown by computational calculations [169]. For instance, the geometry of compound Cp*(PMe₃)Ir(H)₂AlPh₃ indicates that the Ir center in Cp*(PMe₃)Ir is Lewis basic, forming a dative two-electron bond to the aluminum center. This finding strongly contrasts with the bonding situation observed in alylene complexes such as [(CO)₄Fe(AlCp*)], where the electron transfer goes from the Lewis basic, two-electron donor alanediyI Cp*Al to the electron deficient Fe(CO)₄ fragment [147].

Terminally bound alanylene complexes of the type L_nM–AlR₂ contain an electron-deficient Al center that, in principle, may act as a Lewis acid moiety. Such complexes therefore tend to form intra- or intermolecularly coordinated structures as observed in base-stabilized complexes such as [(η⁵-C₅H₅)(CO)₂Fe–Al(CH₂)₃NMe₂]*i*-Bu] and in dimeric complexes such as [(C₅H₄Me)(μ-η¹:η⁵-C₅H₃Me)Mo(μ-Al(H)*i*-Bu)]. Compound [Cp(CO)₂Fe–Al(tmp)₂] is the only

Table 9 M–Al bond lengths (Å) in organoaluminum complexes with d-block metals

Complex	Al–M (Å)	Reference
<i>Alane (AlR₃) complexes</i>		
[Cp*(PMe ₃)(H ₂)Ir–AlPh ₃]	2.684(2)	[147]
[Cp(CO) ₂ Fe–AlPh ₃][NEt ₄]	2.510(2)	[146]
[(Cy ₃ P) ₂ Pt–AlCl ₃]	2.3857(7)	[148]
<i>Alanyle complexes with terminal AlR₂ groups</i>		
[Cp(CO) ₂ Fe–Al(tmp) ₂]	2.450(1)	[153]
[(η^5 -C ₅ H ₅)(CO) ₂ Fe–Al(CH ₂) ₃ NMe ₂] <i>i</i> -Bu]	2.456(1)	[165]
<i>Alanyle complexes with bridging AlR₂ groups</i>		
[{(C ₅ H ₄) ₂ MoAl ₂ Me ₃] ₂]	2.685(3), 2.656(3)	[166]
[(C ₅ H ₅)(C ₅ H ₄) ₂ (H)MoAl ₃ Me ₅]	2.650(5), 2.657(4), 2.951(4), 2.996(5)	[166]
[(C ₅ H ₅)(C ₅ H ₄) ₂ (H)MoAl ₃ Me ₅]	2.662(6), 2.655(5), 2.944(6), 3.003(6)	[167]
[{(C ₅ H ₄ Me)(μ - η^1 : η^5 -C ₅ H ₃ Me)Mo(μ - Al(H) <i>i</i> -Bu)]	2.636(2), 2.944(2)	[154]
[L ₂ Cr ₂ (μ -CH ₃)(μ -AlMe ₂)]	2.8945(14), 2.9076(14)	[164]
<i>Homoleptic alylene complexes with terminal alanediylys (AlR)</i>		
[Pd(AlCp*) ₄]	2.2950(9)	[160]
[Ni(AlCp*) ₄]	2.1727(8)	[160]
[Fe(AlCp*) ₅] ^a	2.2124(15), 2.2419(15), 2.2404(15), 2.3686 (15), 2.3272(14)	[135]
[Fe(AlCp*) ₅] ^a	2.223, 2.378, 2.405, Fe1–Al4 2.444, 2.263	[135]
[Ru(AlCp*) ₅] ^b	2.294(2), 2.331(2), 2.337(2), 2.49(3), 2.434(2)	[135]
<i>Heteroleptic alylene complexes with terminal alanediylys (AlR)</i>		
[(CO) ₄ Fe(AlCp*)]	2.231(3)	[151]
[(CO) ₅ Cr(AlCp*)]	2.3761(6)	[157]
[(dcpe)Pt(AlCp*) ₂]	2.327(2), 2.335(2)	[158]
[(dvds)Pd{Al(ddd)}]	2.3702(10)	[162]
[(Cp*Al) ₃ Ni(μ^2 -H)Al(Ph)Cp*]	2.2105(11), 2.2062(10), 2.1688(11), 2.2912 (11)	[134]
[(Cp*Al) ₃ Ni(H)SiEt ₃]	2.203(8), 2.208(10), 2.180(7)	[134]
[(DippNanacAl)Pd ₂ (μ^2 - GaCp*) ₂ (GaCp*) ₂]	2.456(3), 2.559(3)	[161]
<i>Base-stabilized heteroleptic alylene complexes with terminal alanediylys (AlR)</i>		
[(CO) ₅ W–Al(<i>t</i> -Bu)(tmpda)]	2.741(4)	[152]
[(CO) ₅ Cr–Al(Cl)(tmpda)]	2.482(1)	[152]
[(CO) ₅ W–Al(Et)(tmeda)]	2.670(1)	[168]
[(CO) ₅ W–Al(Cl)(tmpda)]	2.645(2)	[168]
<i>Alylene complexes with bridging alanediylys (AlR)</i>		
[(CpNi) ₂ (μ^2 -AlCp*) ₂]	2.274(2), 2.283(2)	[155]
[(CO) ₆ Co ₂ (μ^2 -AlCp*) ₂]	2.384(3), 2.369(3)/2.377	[156]
[Pt ₂ (GaCp*) ₂ (μ^2 -AlCp*) ₃]	2.3310(7), 2.4259(16), 2.4237(17)	[159]
[{Pd(dvds)} ₂ { μ^2 -AlDippNacnac}]	2.4234(18), 2.4419(18)	[161]
[{Cp*Ir(PMe ₃)(μ^2 -AlEt)} ₂]	2.456(1), 2.459(1)	[147]
[{Cp*(η^2 -C ₂ H ₄)Co(μ -AlEt)} ₂]	2.336(2), 2.333(1)	[163]
[CpFe(CO) ₂] ₂ Al(2-Me ₂ NCH ₂ C ₆ H ₄)]	2.468(1), 2.496(1)	[150]

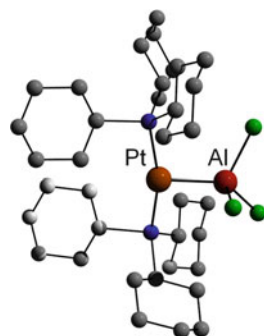
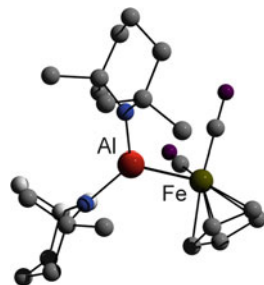
(continued)

Table 9 (continued)

Complex	Al–M (Å)	Reference
<i>Alylene complexes with terminal and bridging alane-diyls (AIR)</i>		
$[\text{Pd}_3(\text{AlCp}^*)_2(\mu^2\text{-AlCp}^*)_2(\mu^3\text{-AlCp}^*)_2]$	2.592(5), 2.498(5), 2.563(5), 2.488(5), 2.401(5), 2.369(5)	[159]
$[\text{Pd}_2(\text{AlCp}^*)_2(\mu^2\text{-AlCp}^*)_3]$	2.3230(18), 2.4559(18), 2.4559(18)	[159]

^aTwo C–H activated isomers containing a μ^2 -bridging Fe–H–Al unit

^bC–H activated isomer containing a μ^2 -bridging Ru–H–Al unit

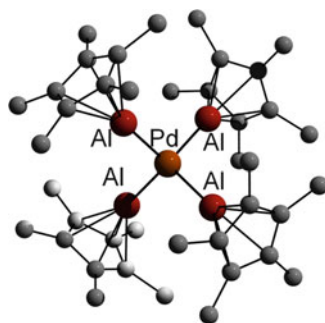
Fig. 21 Solid state structure of $(\text{Cy}_3\text{P})_2\text{Pt–AlCl}_3$ **Fig. 22** Solid state structure of $[\text{Cp}(\text{CO})_2\text{Fe–Al}(\text{tmp})_2]$ 

structurally characterized alanyne complex containing a planar and three-coordinate Al center (Fig. 22).

Thus far reported homoleptic transition metal alkyne complexes of the type $[\text{M}(\text{AlCp}^*)_x]$, which contain terminal alane-diyls Cp^*Al , incorporate up to four Cp^*Al moieties acting as ligands toward transition metal centers. This has been observed with d^{10} metal complexes through the synthesis of $[\text{Ni}(\text{AlCp}^*)_4]$ and $[\text{Pd}(\text{AlCp}^*)_4]$ (Fig. 23). For the d^8 metal complexes, attempted preparations of the $[\text{Fe}(\text{AlCp}^*)_5]$ and $[\text{Ru}(\text{AlCp}^*)_5]$ derivatives, for which a trigonal bipyramidal structure was predicted [13], only yielded undesired C–H activation products. The hypothetical structure $[\text{Fe}(\text{AlCp}^*)_5]$ containing five Fe–Al bonds and bearing unactivated and terminal Cp^* ligands appears unrealistic [135].

In contrast, compound $[(\text{Ph}_3\text{P})_4\text{RuCl}_2]$ reacts with six equivalents GaCp^* to afford $[\text{Ru}(\text{GaCp}^*)_6\text{Cl}_2]$, in which the Ru(II) center is surrounded by six GaCp^*

Fig. 23 Solid state structure of $[\text{Pd}(\text{AlCp}^*)_4]$



moieties and two bridging chloride ligands connect the two Ga centers to one another, hence blocking any C–H activation reactions [170]. The formation of $[\text{Ru}(\text{GaCp}^*)_6\text{Cl}_2]$ from $[(\text{Ph}_3\text{P})_4\text{RuCl}_2]$ results from the substitution of four phosphine ligands by four Cp^*Ga ligands, while two Cp^*Ga groups insert into the Ru–Cl bonds.

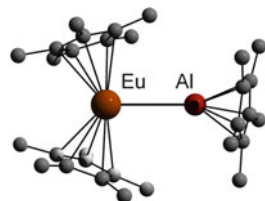
In addition to homoleptic complexes, a large number of heteroleptic alkyne complexes of the type $\text{L}_n\text{M}(\text{AlR})_x$ have been structurally characterized, with the aluminum center bearing a Cp^* , a β -diketiminate, or an alkyl ligand. Lewis-base stabilized heteroleptic complexes of the type $\text{L}_n\text{M}-\text{ECl}(\text{base})$ have also been reported. Unlike Cp^*Al complexes, where the M–Al– Cp^* moiety is almost linear, the M–Al–X angle significantly deviates from linearity in base-stabilized complexes such as $[(\text{CO})_5\text{W}-\text{Al}(\text{Et})(\text{tmeda})]$ ($121.4(2)^\circ$) and $[(\text{CO})_5\text{W}-\text{Al}[(\text{Cl})(\text{tmpda})]]$ ($124.2(1)^\circ$). According to theoretical calculations, the dissociation energies (D_e) of the W–Al bond in species of the type $[(\text{OC})_5\text{W}-\text{AlX}(\text{NH}_3)_2]$ ($\text{X} = \text{H}$ 100.9 kcal/mol, Cl 93.1 kcal/mol) essentially depend on the nature of the Al–X substituent. Replacement of an hydride by a chloride increases the s-character of the Al-based electron lone pair, which decreases donor–acceptor interactions. This goes along with a weakening of the Al–W bond strength because the Al-based donor orbital is more compact. Yet, the W–Al bond in $[(\text{OC})_5\text{W}-\text{AlCl}(\text{NH}_3)_2]$ is shorter than that in $[(\text{OC})_5\text{W}-\text{AlH}(\text{NH}_3)_2]$. Comparable trends were experimentally observed for $[(\text{CO})_5\text{W}-\text{Al}[(\text{Cl})(\text{tmpda})]]$ (2.645(2) Å) and $[(\text{CO})_5\text{W}-\text{Al}(\text{Et})(\text{tmeda})]$ (2.670(1) Å) [168].

The bonding properties of the presently discussed alkyne complexes have been exhaustively studied via quantum chemical calculations. Monovalent group 13 diyls RE are formally isolobal with carbon monoxide CO, phosphanes PR_3 and singlet carbenes CR_2 . Since the HOMO of Cp^*E predominantly consists of a large lobe on E pointing away from the Cp^* ligand, Cp^*E -type species exhibit σ -donor properties as already mentioned. Moreover, the presence of two orthogonal and degenerate LUMOs, which are π -antibonding with respect to the $\text{Cp}^*\text{--E}$ bond, should in principle allow for π -acceptor properties. However, numerous theoretical calculations both on neutral and cationic transition metal complexes of group 13 diyls ER ($\text{E} = \text{B--Tl}$; $\text{R} = \text{H}$, alkyl, aryl, Cp, silyl, amide, halide) clearly demonstrated that the diyls ER are strong σ -donating Lewis bases with rather

Fig. 24 Synthesis of complexes containing group 13/4f metal bonds



Fig. 25 Solid state structure of $[\text{Cp}^*_2\text{Eu}(\text{AlCp}^*)]$



weak π -accepting properties. As expected, the nature of the supporting ligand directly influences the donating/accepting abilities of the metal center. For instance, β -diketiminato-substituted diyls were found to be more Lewis basic than Cp^* -substituted diyls, which is most likely due to the increased negative charge at the gallium atom on the latter [9, 12, 13, 158, 168, 171–175]. An in-depth analysis of the bonding situation in these complexes revealed that ionic contributions may also play an important role in the stability of these bimetallic entities. For instance, while the Al–Fe bond in $[(\text{CO})_4\text{Fe}(\text{AlCp}^*)]$ [151] was initially described as a simple donor–acceptor single bond between the Al(I) center and the Fe(0) atom, subsequent DFT calculations were consistent with a more polar Fe–Al bond ($\text{RAl}^{2+}\text{Fe}(\text{CO})_4^{2-}$) arising from a significant electron transfer from the Al atom to the transition metal center [156].

5 Organoaluminum Complexes with f-Block Metals

Unlike their well-established p- and d-block analogues, f-block metal complexes with direct f-element–Al metal bonds remain extremely rare. However, interest in such derivatives has grown in recent years and initial results on that matter were recently reviewed [176, 177].

The first complexes containing group 13 metal–f-element bonds were reported in 2006 [178]. Lewis acid–base adducts of the type $[\text{Cp}^*_2\text{Ln}(\text{AlCp}^*)]$ ($\text{Ln} = \text{Eu}$ or Yb) (Fig. 25) with direct aluminum(I)–lanthanide(II) bonds were prepared via a solvent-free route involving the reaction of $[\text{Cp}^*\text{Al}]_4$ with a divalent lanthanocene Cp^*_2Ln ($\text{Ln} = \text{Eu, Yb}$) in an evacuated glass ampule at 120°C (Fig. 24). Both lanthanide products dissociate in solution, indicating rather weak donor–acceptor interactions. The oxidation states of the metal centers are consistent with those of the starting complexes. DFT studies showed that the aluminum–4f-element bond in these adducts (about 30 kJ/mol) is essentially electrostatic with little charge transfer and covalent contributions.

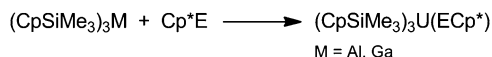


Fig. 26 Synthesis of group 13 diyl-uranium complexes

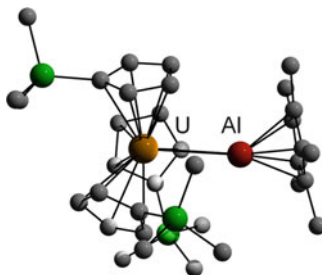


Fig. 27 Solid state structure of $[(\text{CpSiMe}_3)_3\text{U}(\text{AlCp}^*)]$

In addition, the formation of adduct complexes upon reaction of trivalent lanthanides with Cp^*E ($\text{E} = \text{Al}, \text{Ga}$) was proven experimentally. $(\text{CpSiMe}_3)_3\text{Ce}-\text{ECp}^*$ complexes were observed in solution by variable-temperature paramagnetic NMR spectroscopy. Computational calculations using the model complexes $\text{Cp}_3\text{Ln}-\text{ECp}$ ($\text{Ln} = \text{La}-\text{Lu}$; $\text{E} = \text{Al}, \text{Ga}$) agree with shorter $\text{Ln}-\text{E}$ bond distances across the Ln series. These theoretical studies also suggest the $\text{Ln}-\text{E}$ bond to be stronger for Al vs. Ga adduct, unlike earlier reports on divalent lanthanide analogous complexes. Also, the $\text{Nd}-\text{Al}$ bond dissociation energy (BDE) was found to be lower than the energy required (per Al) to disrupt the competitively formed $(\text{Cp}^*\text{Al})_4$ tetramer. Therefore $(\text{CpSiMe}_3)_3\text{Nd}-\text{AlCp}^*$ was predicted not to be isolable. The highest BDE was calculated for the $\text{CpE}-\text{Gd}$ donor-acceptor interaction. According to these calculations, the $\text{Ln}-\text{E}$ bonding interactions are predominantly covalent with a nonpolar donor-acceptor character; the formation of a strong covalent bond is not observed because of resistance to reduction of an effectively divalent Ln center [179].

Group 13-actinide complexes have been even less studied thus far than lanthanide complexes. The $\text{U}-\text{Al}$ compound $[(\text{CpSiMe}_3)_3\text{U}(\text{AlCp}^*)]$, arising from the reaction of Cp^*Al with $(\text{CpSiMe}_3)_3\text{U}$, constitutes the first structurally characterized $\text{U}-\text{Al}$ complex [180] (Fig. 26).

In compound $[(\text{CpSiMe}_3)_3\text{U}(\text{AlCp}^*)]$ (Fig. 27), the $\text{U}-\text{Al}$ bond lengths of two crystallographically inequivalent molecules (3.117(3), 3.124(4) Å) are very close to the sum of the covalent radii. A calculated natural charge of 0.540 (0.560) for the AlCp fragment hints toward a small $\text{Al}-\text{U}$ net charge transfer of 0.091. The Wiberg bond index between U and Al indicates a covalent bond order of ca. 0.5.

Arnold et al. also performed theoretical calculations to compare intermetallic group 13 metal complexes of 4f and 5f metals, these being synthesized by reaction of $(\text{CpSiMe}_3)_3\text{Nd}$ and $(\text{CpSiMe}_3)_3\text{U}$ with Cp^*E ($\text{E} = \text{Al}, \text{Ga}$) [181]. While the uranium complexes were isolated on gram scales and characterized by single crystal X-ray diffraction, the Nd analogues were only observed spectroscopically.

DFT calculations revealed that Cp*Al is a slightly better donor than Cp*Ga, while U is a better acceptor than Nd for soft σ -donating ligands (by an order of magnitude) according to quantitative ^1H NMR studies. As a consequence, some gallanediyl complexes of 4f and 5f elements have been synthesized in the past [182–185]. Moreover, Cp*Al and Cp*Ga are both capable of binding 5f over 4f elements with an excellent selectivity, which, according to DFT calculations, primarily results from a strong σ -interaction. These calculations also excluded a stabilization of the 5f electrons (of the U metal center) through π -backbonding.

6 Conclusions and Outlook

The synthesis of monovalent alane-diyls of the type AlR, behaving as excellent σ -donor properties, has opened the way to the synthesis of a large variety of intermetallic complexes including p-block, d-block and, to a lesser extent thus far, f-block metals. The derived organometallic complexes display a fascinating structural diversity and, in some instances, exhibit unprecedented chemical reactivity due to their interesting bonding properties. In such species, fine tuning of the group 13 metal-bound ligands allow further adjustments of the σ -donor/ π -acceptor properties, hence enabling the synthesis of novel intermetallic complexes in the near future. In this regard, structurally characterized intermetallic organocompounds incorporating a direct Al–s-block–metal bond, unknown to date, would be of particular interest.

References

1. He N, Xie H-B et al (2007) *Organometallics* 26:6839
2. Fedushkin IL, Lukoyanov AN et al (2008) *Chem Eur J* 14:8465
3. Fedushkin IL, Lukoyanov AN et al (2010) *Chem Eur J* 16:7563
4. Bonello O, Jones C et al (2010) *Organometallics* 29:4914
5. Wieko M, Roesky PW et al (2007) *Chem Commun* 927
6. Liu Y, Li S et al (2011) *J Organomet Chem* 696:1450
7. Schumann H, Hummert M et al (2007) *Chem Eur J* 13:4216
8. Fischer RC, Power PP (2010) *Chem Rev* 110:3877
9. Macdonald CLB, Cowley AH (1999) *J Am Chem Soc* 121:12113
10. Timoshkin AY, Frenking G (2002) *J Am Chem Soc* 124:7240
11. Cowley AH (2004) *Chem Commun* 2369
12. Uddin J, Boehme C et al (2000) *Organometallics* 19:571
13. Uddin J, Frenking G (2001) *J Am Chem Soc* 123:1683
14. Gordon JD, Voigt A et al (2000) *J Am Chem Soc* 122:950
15. Jutzi P, Neumann B et al (2001) *Organometallics* 20:2854
16. Hardman NJ, Power PP et al (2001) *Chem Commun* 1866
17. Yang Z, Ma X et al (2005) *Angew Chem Int Ed* 44:7072
18. Hardman NJ, Wright RJ et al (2003) *J Am Chem Soc* 125:2667
19. Wright RJ, Phillips AD et al (2002) *J Am Chem Soc* 124:8538
20. Frenking G, Fröhlich N (2000) *Chem Rev* 100:717
21. Rayon VM, Frenking G (2002) *Chem Eur J* 8:4693–4707

22. Gorden JD, MacDonald CLB et al (2001) *Chem Commun* 75
23. Schulz S, Kuczkowski A et al (2006) *Organometallics* 25:5487
24. Lammertsma K, Güner OF et al (1989) *Inorg Chem* 28:313
25. Gordon JD, MacDonald CLB et al (2005) *Main Group Chem* 4:33
26. Dohmeier C, Robl C et al (1991) *Angew Chem Int Ed* 30:564
27. Haaland A, Martinsen K-G et al (1995) *Organometallics* 14:3116
28. Loos D, Baum E et al (1997) *Angew Chem Int Ed* 36:860
29. Haaland A, Martinsen K-G (1994) *Acta Chem Scand* 48:172
30. Beachley OT Jr, Blom R et al (1989) *Organometallics* 8:346
31. Romero PE, Piers WE et al (2003) *Organometallics* 22:1266
32. Haaland A (1989) *Angew Chem Int Ed* 28:992
33. Haaland A (1993) Normal and dative bonding in neutral aluminum compounds. In: Robinson GH (ed) *Coordination chemistry of aluminum*. VCH, Weinheim
34. Jones AC (1997) *Chem Soc Rev* 101
35. Jegier JA, Gladfelter WL (2000) *Coord Chem Rev* 206–207:631
36. Carmalt CJ, Basharat S (2007) Precursors to semiconducting materials. In: O'Hare D (ed) *Comprehensive organometallic chemistry III*, 12.01:1. Elsevier, Amsterdam
37. Malik MA, Afzaal M et al (2010) *Chem Rev* 110:4417
38. Wiberg E, May A (1955) *Z Naturforsch B* 10:229
39. Staubitz A, Robertson APM et al (2010) *Chem Rev* 110:4079
40. Welch GC, San Juan RR et al (2006) *Science* 314:1124
41. Stephan DW, Erker G (2010) *Angew Chem Int Ed* 49:46
42. Staubitz A, Robertson APM et al (2010) *Chem Rev* 110:4023
43. Romm IP, Noskov YG et al (2007) *Rus Chem Bull Internat Ed* 56:1935
44. Schulz S (2003) *Adv Organomet Chem* 49:225
45. Spiridonov A, Malkova AS (1969) *Zh Strukt Khim* 10:33; *J Struct Chem USSR* 10:303
46. Coleman AP, Nieuwenhuyzen M et al (1995) *Chem Commun* 2369
47. Malkova AS, Suvorov AV (1969) *Russ J Inorg Chem* 14:1049
48. Kutzelnigg W (1984) *Angew Chem Int Ed* 23:272
49. Schulz S, Nieger M (1999) *Organometallics* 18:315
50. Nieger M, Schulz S Private communication, Cambridge Crystallographic Data Center, CCDC No. 138649
51. Schulz S, Kuczkowski A et al (2000) *J Organomet Chem* 604:202
52. Schulz S, Kuczkowski A et al (2010) *J Organomet Chem* 695:2281
53. Schuchmann D, Kuczkowski A et al (2007) *Eur J Inorg Chem* 931
54. Kuczkowski A, Schulz S et al (2001) *Eur J Inorg Chem* 2605
55. Kuczkowski A, Fahrenholz S et al (2004) *Organometallics* 23:3615
56. Kuczkowski A, Heimann S et al (2011) *Organometallics* 30:4730
57. Kuczkowski A, Schulz S et al (2001) *Organometallics* 20:2000
58. Kuczkowski A, Schulz S et al (2001) *Angew Chem Int Ed* 40:4222
59. Kuczkowski A, Schulz S et al (2002) *Organometallics* 21:1408
60. Ashe AJ III, Ludwig EG Jr et al (1984) *Organometallics* 3:337
61. Mundt O, Riffel H et al (1984) *Z Naturforsch* 39b:317
62. Pykkö P, Atsumi M (2009) *Chem Eur J* 15:186
63. Samaan S (1978) *Metallorganische Verbindungen des Arsens, Antimons und Bismuts*. In: Houben Weyl, *Methoden der Organischen Chemie*, 4th edn. Thieme Verlag, Stuttgart
64. Keys A, Brain PT et al (2008) *Dalton Trans* 404
65. Woski M, Mitzel NW (2004) *Z Naturforsch* 59b:269
66. Cowley AR, Downs AJ et al (2005) *Organometallics* 24:5702–5757
67. Schulz S, Nieger M (1998) *Organometallics* 17:3398
68. Matar M, Kuczkowski A et al (2007) *Eur J Inorg Chem* 2472
69. Schulz S, Kuczkowski A et al (2000) *Organometallics* 19:699
70. Schulz S, Nieger M (1999) *Angew Chem Int Ed* 38:967

71. Barron AR, Cowley AH et al (1988) *Polyhedron* 7:77
72. Cowley AH, Jones RA et al (1988) *J Organomet Chem* 341:C1
73. Cowley AH, Jones RA et al (1990) *Chem Mater* 2:221
74. Baldwin RA, Foos EE et al (1996) *Organometallics* 15:5035
75. Wells RL, Foos EE et al (1997) *Organometallics* 16:4771
76. Schulz S, Nieger M (1998) *J Organomet Chem* 570:275
77. Foos EE, Wells RL et al (1999) *J Cluster Sci* 10:121
78. Foos EE, Jouet RJ et al (1999) *J Organomet Chem* 582:45
79. Foos EE, Jouet RJ et al (2000) *J Organomet Chem* 598:182
80. Lide DR (1997–1998) *CRC handbook of chemistry and physics*, 78th edn. CRC, New York, p 9
81. Schulz S, Nieger M (2002) *Organometallics* 21:2793
82. Schulz S, Schoop T et al (1995) *Angew Chem Int Ed* 34:919
83. Breunig HJ, Stanciu M et al (1998) *Z Anorg Allg Chem* 624:1965
84. Thomas F, Schulz S et al (2003) *Organometallics* 22:3471
85. Thomas F, Schulz S et al (2003) *Angew Chem Int Ed* 42:5641
86. Schulz S, Thomas F et al (2006) *J Chem Soc Chem Commun* 1860
87. Schulz S (2003) *Adv Organomet Chem* 49:225
88. Schulz S (2002) Synthesis, structure and reactivity of group 13/15 compounds containing the heavier elements of group 15. In: Roesky HW, Atwood DA (eds) *Structure and bonding. Group 13 chemistry I: fundamental new developments*, vol 103, p 117
89. Thomas F, Schulz S et al (2002) *Z Anorg Allg Chem* 628:235
90. Schulz S, Nieger M (2000) *Organometallics* 19:2640
91. Schulz S, Thomas F et al (2000) 19:5758
92. Thomas F, Schulz S et al (2001) *Eur J Inorg Chem* 161
93. Schulz S, Nieger M (2011) *J Chem Crystallogr* 41:349
94. Atwood DA, Contreras L (1993) *Organometallics* 12:17
95. Janik JF, Wells RL (1998) *Inorg Chem* 37:3561
96. Wang Y, Xie Y et al (2004) *Science* 321:1069
97. Wang Y, Robinson GH (2011) *Inorg Chem* 50:12326
98. Wang Y, Robinson GH (2012) *J Chem Soc Dalton Trans* 41:337
99. Wang Y, Robinson GH (2009) *Chem Commun* 5201
100. Vogel U, Timoshkin AY et al (2001) *Angew Chem Int Ed* 40:4409
101. Thomas F, Schulz S et al (2002) *Chem Eur J* 8:1915
102. Thomas F, Schulz S et al (2001) *Organometallics* 20:2405
103. Bodner GM, May MP et al (1980) *Inorg Chem* 19:1951
104. Tessier-Youngs C, Bueno C et al (1983) *Organometallics* 7:1054
105. Veith M, Frank W (1985) *Angew Chem Int Ed* 24:223
106. Veith M, Recktenwald O (1982) *Top Curr Chem* 104:1–55 (Springer, New York)
107. Cowley AH, Jones RA et al (1991) *Angew Chem Int Ed* 30:1143
108. Harlan CJ, Gillan EG (1996) *Organometallics* 15:5479
109. Cui C, Roesky HW et al (1999) *Organometallics* 18:5120
110. Cui C, Roesky HW et al (2000) *Inorg Chem* 39:3678
111. Klimek KS, Proust J et al (2001) *Organometallics* 20:2047
112. Zheng W, Mösch-Zanetti NC et al (2000) *Angew Chem Int Ed* 39:4276
113. Jancik V, Moya Cabrera MM (2004) *Eur J Inorg Chem* 3508
114. Gardiner MG, Raston CL et al (1995) *J Chem Soc Chem Commun* 2501
115. Schulz S, Roesky HW et al (1993) *Angew Chem Int Ed* 32:1729
116. Uhl W, Schütz U (1994) *Z Naturforsch* 49b:931
117. Barden CJ, Charbonneau P et al (2002) *Organometallics* 21:3605
118. Godfrey PD, Raston CL et al (1997) *Chem Commun* 2235
119. Gardiner MG, Raston CL et al (1995) *J Chem Soc Chem Commun* 1457
120. Kuchta MC, Parkin G (1998) *Coord Chem Rev* 176:323
121. Gillan EG, Barron AR (1997) *Chem Mater* 9:3037

122. Garje SS, Copsey MC et al (2006) *J Mater Chem* 16:4542
123. Corradine P, Sirrigu A (1967) *Inorg Chem* 6:601
124. Schwarzhans E, Steiger H (1972) *Angew Chem Int Ed* 11:535
125. Kroll WR, McVicker GB (1971) *J Chem Soc D* 591
126. Schrieke RR, Smith JD (1971) *J Organomet Chem* 31:C46
127. Tebbe FN, Guggenberger LJ (1973) *J Chem Soc Chem Commun* 227
128. Schneider JJ, Denninger U et al (1994) *Z Naturforsch* 49b:1549
129. Conway AJ, Gainsford GJ et al (1975) *J Chem Soc Dalton Trans* 2499
130. Gainsford GJ, Schrieke RR et al (1972) *J Chem Soc Chem Commun* 650
131. Su J, Li X-W et al (1997) *Organometallics* 16:4511
132. Cotton FA, Feng X (1998) *Organometallics* 17:128
133. Dagani R (1998) *Chem Eng News* 76:31
134. Steinke T, Gemel C et al (2004) *Angew Chem Int Ed* 43:2999
135. Steinke T, Cokoja M et al (2005) *Angew Chem Int Ed* 44:2943
136. Cadenberg T, Gemel C et al (2005) *J Am Chem Soc* 127:17068
137. Fischer RA, Miehr A (1996) *Chem Mater* 8:497
138. Cokoja M, Parala H et al (2006) *Chem Mater* 18:1634
139. Cokoja M, Jagirdar BR et al (2008) *Eur J Inorg Chem* 3330
140. Cokoja M, Parala H et al (2007) *Chem Mater* 19:5721
141. Fischer RA, Weiß J (1999) *Angew Chem Int Ed* 38:2830
142. Linti G, Schnöckel H (2000) *Coord Chem Rev* 206–207:285
143. Gemel C, Steinke T et al (2004) *Eur J Inorg Chem* 4161
144. Marciniec B, Pawluc P et al (2007) *Inorganometallic Chemistry*. In: Bertini E (ed) *Inorganic and bio-inorganic chemistry*, vol 1. *Encyclopedia of Life Support Systems (EOLSS)*, Developed under the Auspices of the UNESCO, Eolss Publishers, Oxford, p 239 ff. <http://www.eolss.net>. Retrieved 7 Sep 2011
145. Bollermann T, Cadenbach et al (2011) *Inorg Chem* 50:5808
146. Burlitch JM, Leonowicz ME et al (1979) *Inorg Chem* 18:1097
147. Golden JT, Peterson TH et al (1998) *J Am Chem Soc* 120:223
148. Braunschweig H, Gruss K et al (2007) *Angew Chem Int Ed* 46:7782
149. Amgoune A, Bourissou D (2011) *J Chem Soc Chem Commun* 47:859
150. Braunschweig H, Müller J et al (1996) *Inorg Chem* 35:7443
151. Weiß J, Stetzkamp D et al (1997) *Angew Chem Int Ed* 36:70
152. Fölsing H, Segnitz O et al (2000) *J Organomet Chem* 606:132
153. Anand BN, Krossing I et al (1997) *Inorg Chem* 36:1979
154. Stender M, Oesen H et al (2001) *Z Anorg Allg Chem* 627:980
155. Dohmeier C, Krautscheid H (1994) *Angew Chem Int Ed* 33:2482
156. Üffing C, Ecker A et al (1998) *Organometallics* 17:2373
157. Yu Q, Purath A et al (1999) *J Organomet Chem* 584:94
158. Weiß D, Steinke T et al (2000) *Organometallics* 19:4583
159. Steinke G, Gemel C et al (2005) *Chem Eur J* 11:1636
160. Buchin B, Steinke T et al (2005) *Z Anorg Allg Chem* 631:2756
161. Kempter A, Gemel C et al (2006) *Chem Commun* 1551
162. Kempter A, Gemel C et al (2007) *Chem Eur J* 13:2990
163. Schneider JJ, Krüger C (1994) *Angew Chem Int Ed* 33:2435
164. Noor A, Glatz G et al (2009) *Nature Chem* 1:322
165. Fischer RA, Priemeier T (1994) *Organometallics* 13:4306
166. Forder RA, Prout K (1974) *Acta Cryst* B30:2312
167. Rettig SJ, Storr A et al (1974) *Acta Cryst* B30:666
168. Fischer RA, Schulte MM et al (1998) *J Am Chem Soc* 120:1237
169. Tsukamoto S, Sakaki S (2011) *J Phys Chem A* 115:8520
170. Cadenbach T, Gemel C et al (2004) *J Chem Soc Dalton Trans* 3171
171. Doerr M, Frenking G (2002) *Z Anorg Allg Chem* 628:843

172. Coombs ND, Clegg W et al (2008) *J Am Chem Soc* 130:5449
173. Vidovic D, Aldridge S (2011) *Chem Sci* 2:601
174. Pandey KK, Braunschweig H et al (2011) *Inorg Chem* 50:1402
175. Pandey KK, Aldridge S (2011) *Inorg Chem* 50:1798
176. Liddle ST (2009) *Proc R Soc A* 465:1673
177. Roesky PW (2009) *J Chem Soc Dalton Trans* 1887
178. Gamer MT, Roesky PW et al (2006) *Angew Chem Int Ed* 45:4447
179. Krinsky JL, Minasian SG et al (2011) *Inorg Chem* 50:345
180. Minasian SG, Krinsky JL et al (2008) *J Am Chem Soc* 130:10086
181. Minasian SG, Krinsky JL et al (2009) *J Am Chem Soc* 131:13767
182. Wiecko M, Roesky PW (2007) *Organometallics* 26:4846
183. Arnold PL, Liddle ST et al (2007) *J Am Chem Soc* 129:5360
184. Jones C, Stasch A et al (2009) *J Chem Soc Chem Commun* 113
185. Liddle ST, McMaster J et al (2009) *Angew Chem Int Ed* 48:1077

<http://www.springer.com/978-3-642-33671-3>

Modern Organoaluminum Reagents

Preparation, Structure, Reactivity and Use

Woodward, S.; Dagorne, S. (Eds.)

2013, XI, 312 p. 131 illus., 42 illus. in color., Hardcover

ISBN: 978-3-642-33671-3